CHIMIA 45 (1991) Nr. 6 (Juni)

Chimia 45 (1991) 175–190

Chemistry with Red and Near Infrared Light

Heinz Frei*

Abstract. Opportunities are explored to initiate controlled chemistry by photolysis with long-wavelength visible and near infrared light. In one direction, bimolecular reactions are induced by exciting collisional pairs in a solid matrix to energy surfaces well below reactant dissociation limits. Examples discussed include product specific (including stereospecific) photo-oxidation of small alkenes and alkynes by NO_2, and cycloaddition reactions of singlet SO and singlet O_2. Conducting the chemistry in rare gas matrices allows us to elucidate elementary reaction steps by FT-IR spectroscopy of trapped intermediates, and to gain insight into the dynamics of transients by wavelength-dependent laser photochemistry. In the case of olefin epoxidations, stereochemical details of reaction paths are uncovered by chemical trapping of transient oxirane biradicals in their nascent conformation. State-specific reactions of singlet excited SO and singlet O_2 with hydrocarbons illustrate how photons deep in the near infrared can be used for controlled chemical synthesis. In parallel work, excited state redox reactions in homogeneous and colloidal semiconductor solutions are explored that pertain to chemical storage of near infrared quanta and conversion into electrical energy. Examples are studies on chemical storage of singlet delta molecular oxygen ($O_2(^1\Delta)$), a metastable near infrared energy carrier, its excited state redox chemistry in aqueous solution, and direct reduction of $O_2(^1\Delta)$ at a semiconductor electrode. Using very sensitive time resolved optical techniques, new mechanistic insight is gained on singlet O_2 reactions, and on photo-oxidation of halide at the semiconductor-solution interface.

Heinz Frei, a native of Luzern, studied chemistry at ETH Zürich (Abteilung für Naturwissenschaften). He did his thesis at ETH with Prof. *Hs.H. Günthard* on infrared spectroscopic studies of conformational problems (Ph.D. 1977). From 1978 to 1981, he was a fellow of the *Schweizerische Nationalfonds*, working with Prof. *G.C. Pimentel* at the University of California, Berkeley, on vibrationally induced bimolecular reactions in cryogenic matrices. He started his work on near infrared photochemistry after joining the University of California's Lawrence Berkeley Laboratory (1981), where he became Principal Investigator in 1984, and Senior Scientist in 1990. His current research interests focus on controlled photochemical synthesis in solid matrices, and on long wavelength light induced redox reactions in solution.

1. Introduction

Photons as a means to initiate chemistry offer an opportunity to exert product control by furnishing access to selected reaction surfaces. Despite the fact that the principles governing the initial reactive events of photo-excited molecules are not restricted to light of any particular wavelength, chemistry induced by photons in the long-wavelength visible (VIS) and near-IR (NIR) region is expected to exhibit much tighter product control than photochemistry brought about by shorter wavelength, blue or near ultraviolet quanta (NIR defined as the wavelength region between 700 and 2000 nm). One quite general reason is that access is restricted to the lowest excited reaction surface(s), with primary photoproducts emerging with the least amount of excess internal energy, which minimizes the chances of subsequent rearrangement or fragmentation. Moreover, in most cases, long-wavelength VIS and NIR photons do not carry sufficient energy to cause reactant dissociation, hence, if reaction can be initiated by these photons it would occur in the absence of uncontrolled chemistry brought about by atoms or free radical fragments. Yet the special opportunities of reactions induced by (single) long-wavelength photons, particularly those in the NIR for accomplishing controlled chemistry have remained virtually unexplored. While there are always properties unique to the particular system at hand that influence the course of the chemistry, the factors just mentioned give ample incentive to explore low-energy paths of chemical reactions that can be accessed by long-wavelength photons.

Search for new, controlled chemistry with red and NIR light is motivated in particular by a need for substantial progress in the use of solar photon energy for chemical purposes. First, control and specificity are crucial aspects of the efficient use of photon energy. Second, about half (52%) of the solar irradiance at ground level lies at wavelengths longer than 700 nm, a full 75% in the red and NIR region combined [1]. While plant and bacterial photosynthetic systems are well adapted to the spectral distribution of the sun's energy, as they use almost exclusively photons in the deep red and NIR, solar photochemists have thus far paid little attention to reactions that can be induced by quanta of this spectral region. Hence, in our search for chemistry that can be initiated by long-wavelength light we put special emphasis on reactions that may serve as models, or suggest new concepts, for temporary chemical storage of NIR photons, efficient conversion into electricity, for red and NIR light-assisted synthesis of organic building blocks and high valued chemicals from abundant chemicals, and for photocatalysis.

Over the past several years, we have explored low-energy paths of reactions in two different environments, namely cryogenic solid matrices and room-temperature solutions. A solid matrix is a natural environment for controlled bimolecular photochemistry, since reactant nearest neighbors enclosed in a matrix cage are held in contact indefinitely, hence absorption of a photon occurs always, while the partners are in a state of collision. Irradiation *during* a collision is the best way to initiate chemistry of molecules excited to levels below the dissociation threshold as reaction can only occur, if the excitation is sustained up to the moment of collision. Cryogenic inert-gas matrices are a good starting point because the diagnostic tool of *Fourier*-transform IR spectroscopy (FT-IR) of trapped chemical intermediates and wavelength dependent laser photochemistry can be employed to uncover elementary reaction steps and gain insight into the dynamics of transients that dictate the course of the chemistry. Selective vibronic excitation of reactant pairs allows us to learn about the state dependence of the reaction. Monitoring of IR product growth as function of photolysis wavelength can be used as a sensitive spectroscopic tool to identify very weak vibronic states involved in NIR-light-induced chemistry. While work in matrices typically involves atom transfer, addition, and substitution reactions, studies in room-temperature solution give us an opportunity

* *Correspondence*: Dr. H. Frei**
Chemical Biodynamics Division
Lawrence Berkeley Laboratory
University of California, Berkeley, CA 94720, USA
** *Werner Prize* with medal 1990, awarded by the Swiss Chemical Society (SCG)

to explore red and NIR-induced redox chemistry. Emphasis is again on elucidation of elementary reaction steps, since insight gained therefrom is the key to rapid advance to the most interesting chemical systems. Very sensitive time resolved emission and absorption techniques are used as main tools. Long-wavelength-light-induced redox reactions relevant to energy storage and conversion have driving forces that are modest at best, hence mediation of reactions, for example by semiconductor materials, is of particular importance. Experiments in this area focus on real time monitoring of one electron redox intermediates in colloidal semiconductor solutions to determine energetics and kinetics of elementary reaction events at the semiconductor-solution interface.

Red- and NIR-light-induced bimolecular reactions in solid matrices will be discussed in *Sect. 2*. Examples include controlled hydrocarbon photo-oxidations and cycloaddition reactions on low-lying excited surfaces. In *Sect. 3*, time-resolved spectroscopic work on redox reactions in homogeneous and colloidal semiconductor solutions will be presented that pertains to chemical storage of NIR photon energy and conversion into electrical energy.

2. Long Wavelength Light-Induced Chemistry in Solid Matrices

A key step towards controlled bimolecular chemistry is to ensure that no free atoms are generated along the reaction path, since they tend to attack substrate molecules non-specifically, which often results in multiple product branching. Taking oxidation of an olefin by NO_2 as an example to illustrate this point, we would, therefore, seek to initiate O-atom transfer by exciting NO_2 to bound vibronic states below the 398 nm (71.8 kcal mol^{-1}) dissociation limit rather than dissociating it first to $O(^3P)$ ground state atoms and NO by irradiation at photon energies above the 398 nm threshold (*Fig. 1*). Preparation of sustained collisional reactant pairs in a rare gas solid matrix at cryogenic temperature is a convenient approach to explore in detail such large amplitude bimolecular chemistry (as opposed to a dissociation-addition or dissociation-substitution sequence of steps). Photochemistry can be initiated by continuous light sources, and reaction paths mapped by trapping transients and determining their structure by FT-IR spectroscopy. IR absorptions of species embedded in rare gas matrices have narrow widths (on the order of 1 cm^{-1}), which facilitates separation and identification of individual conformers of trapped intermediates and final products [2]. Moreover, measurement of the growth kinetics of IR product absorptions as function of photolysis wavelength allows us to determine the photolysis photon energy dependence of reaction quantum efficiencies and thereby learn about the dynamics of the chemical reaction.

We will discuss in turn three types of red- or NIR-bimolecular reactions in matrices, namely O-atom transfer to small unsaturated hydrocarbons (*2.1*), cycloaddition reactions of singlet SO and singlet O_2 (*2.2*), and other types of reactions of O_2 with inorganic and organic compounds (*2.3*).

2.1. *Photo-oxidation of Unsaturated Hydrocarbons by NO_2*

2.1.1. *Acyclic Alkene + NO_2*

Epoxidation of (*E*)-but-2-ene was our first example of chemistry induced by photoexcitation of matrix isolated NO_2 · hydrocarbon pairs below the NO_2 dissociation limit [3]. (*E*)-butene · NO_2 collisional pairs were prepared in solid matrices by co-depositing gaseous alkene/rare gas and NO_2/rare gas mixtures (rare gas most often Ar) through separate vacuum lines onto a 12 K cooled, IR transparent window (CsI). Concentrations were chosen so that typically 10–20% of the alkene molecules would have a NO_2 nearest neighbor. Since molecules do not undergo diffusion in these solid matrices at 12 K, the reservoir of collisional reactant pairs formed upon deposition is depleted as chemical reaction proceeds. IR spectra are recorded after preparation of the matrix, and following each period of irradiation of the matrix with monochromatic light from continuous wave (cw) Ar ion laser (8 discrete emission lines in the 458–515 nm region), or from an Ar or Kr ion laser pumped cw dye laser (continuously tunable from 520 to 1000 nm). Neither IR nor VIS/NIR spectra revealed any special features of alkene · NO_2 cage pairs that would indicate formation of a complex, hence the designation 'collisional pairs'.

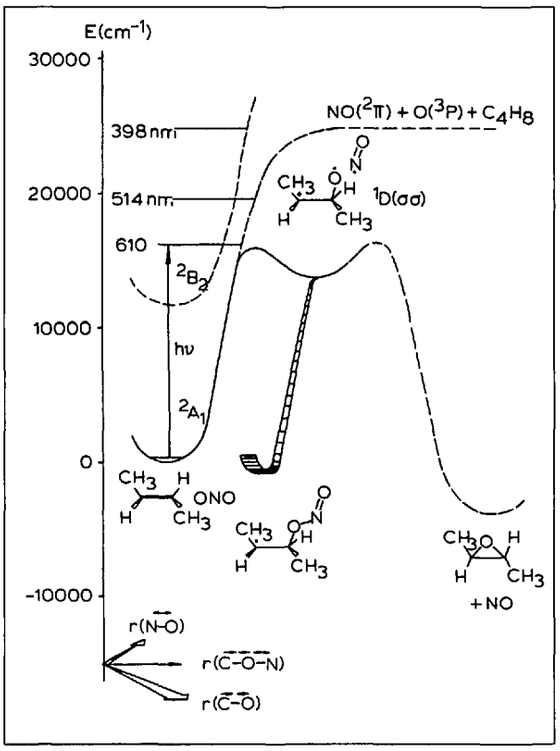

Fig. 1. *Potential energy diagram for but-2-ene + NO_2 reaction.* Energies of stable species are based on available standard enthalpies of formation, the energy of oxirane biradical corresponds to the *ab initio* estimate of the $^1D(\sigma\sigma)$ ground electronic state of CH_2–CH_2–O taken from [7][10].

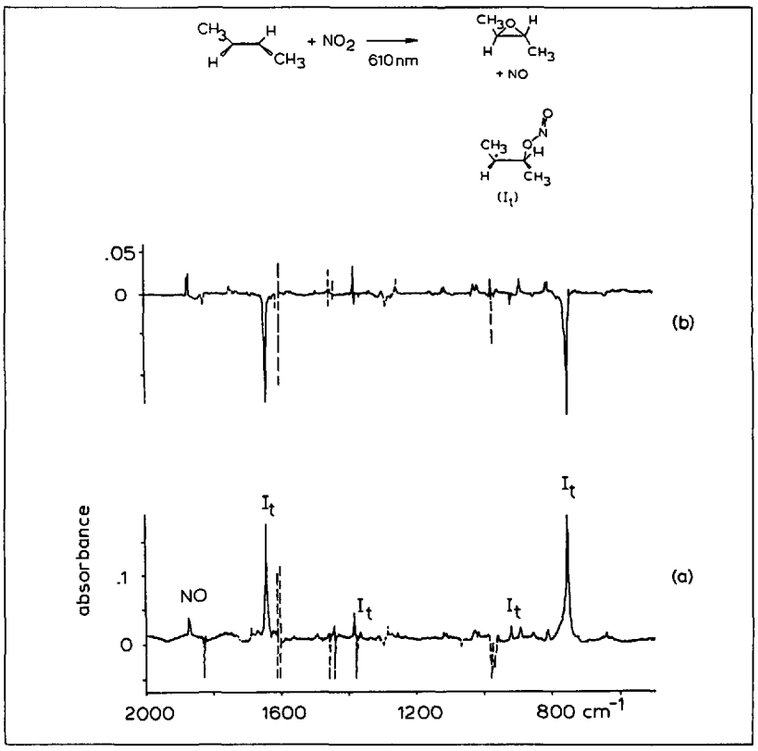

Fig. 2. *a) IR product growth after 60 min irradiation of a matrix* (E)-*but-2-ene*/NO_2/*Ar = 2.5/1/200 at 610 nm.* Bands labelled I_t are attributed to butyl-nitrite radical. All other (solid) bands originate from trans-2,3-epoxybutane (and NO). Dashed absorptions are due to reactants or N_xO_y species [3]. *b) Absorption changes upon 6-min photolysis of sample* (a) *at 514 min.* All I_t absorptions decrease, while those of (*E*)-but-2-ene oxide and NO grow.

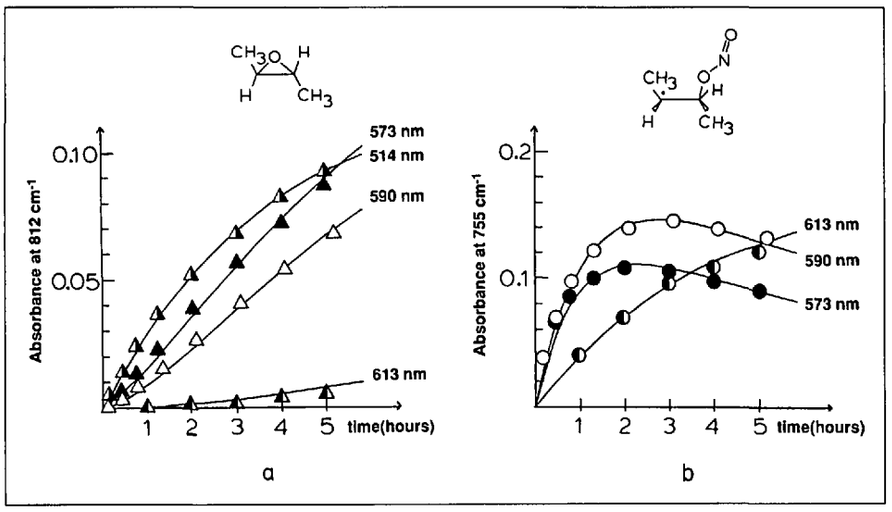

Fig. 3. *Absorbance growth behavior of* (E)*-but-2-ene oxide* (a) *and butyl-nitrite radical* (b) *upon irradiation of matrices* (E)*-but-2-ene*/NO_2/Ar = 2.5/1/100 *at 613 nm* (299 mWcm^{-2}), *590 nm* (405 mWcm^{-2}), *573 nm* (242 mWcm^{-2}), *and 514 nm* (49 mWcm^{-2}). Solid traces represent fits to integrated rate equations [3]. Each curve has been obtained starting with a new matrix.

Since NO_2 has vibronic absorptions throughout the VIS and a large part of the NIR region [4], these tunable light sources could be employed for a search of the precise threshold to reaction. Taking differences of IR spectra recorded before and after irradiation as shown in *Fig. 2a*, we found that 610 nm was the longest wavelength at which chemistry of (*E*)-but-2-ene · NO_2 pairs was initiated. This corresponds to excitation 25 kcal mol^{-1} below the dissociation limit of the reactant (*Fig. 1*). IR spectra revealed that the only final products formed were *trans*-2,3-epoxybutane and NO. No *cis*-diastereoisomer of the epoxide was observed. However, five additional product absorptions appeared that could not be assigned to any known species, with the most prominent bands at 1646 and 755 cm^{-1} as is readily discerned from the spectrum of *Fig. 2a*. After buildup of the new species, we tuned the photolysis laser to a shorter, green wavelength (514 nm) and irradiated for a brief period. This led to complete loss of these five absorptions under concurrent growth of *trans*-epoxide and NO, as shown in the spectrum of *Fig. 2b*. This implies that the new species has the composition $C_4H_8O_2N$. IR analysis based on partial and full ^{18}O isotopic substitution showed unequivocally that it is the butyl nitrite radical CH_3–$\dot{C}H$–$CH(CH_3)$–ONO [3].

To find out whether the final products, epoxide and NO, were not only generated by secondary photolysis of nitrite radical, but also upon direct photo-excitation of (*E*)-but-2-ene · NO_2 pairs, the absorbance growth curves of epoxide and nitrite radical were determined at several photolysis wavelengths, as shown in *Fig. 3*. The epoxide growth upon 613 nm excitation exhibits an induction period (*Fig. 3a*), indicating that at the photolysis threshold epoxide is produced exclusively by secondary photolysis of butyl nitrite radical. On the other hand, epoxide growth upon 590 nm irradiation exhibits a distinct non-zero slope at the beginning of photolysis, which means that (*E*)-but-2-ene oxide is produced directly by single photon excitation of butene · NO_2 pairs as well. The continuing role of secondary photolysis at this shorter wavelength is manifested by the decrease of the nitrite radical curve at long photolysis times (*Fig. 3b*) and by the sigmoidal shape of the epoxide absorbance growth curve (*Fig. 3a*). To determine quantitatively the fraction of epoxide formed upon direct excitation of but-2-ene · NO_2 pairs, analysis of these absorbance growth curves by fitting rate constants k_1, k_2, and k_3 of *Scheme 1* to the corresponding integrated rate laws was required. From such analysis, we found that the epoxide yield upon direct photo-excitation of butene · NO_2 pairs, $k_3/(k_1+k_3)$, increases sharply as the photolysis photon energy is raised from the 610 nm threshold towards shorter, yellow and green wavelengths [3] ($k_3/(k_1+k_3)$ is equal to the relative quantum efficiency to epoxide formation $\phi_3/(\phi_1+\phi_3)$ according to the approximation $k = \varepsilon\phi \cdot I_{laser}$ for the weak absorption limit. ε is the cross section of the absorber, I_{laser} the photolysis light intensity).

Immediate questions raised by these results were: *i*) is the photo-epoxidation induced by red photons not only diastereoselective, but even diastereospecific [5]? *ii*) Is the observed butyl-nitrite radical formed along a reaction path completely separate from that of epoxide formation (*e.g.* by direct electrophilic addition of NO_2 to the C=C bond), or does its path share a common reaction step with the O atom transfer path that leads to epoxide? In the latter case, the conformation of the butyl nitrite radical might furnish insight into the detailed stereochemical path of alkene epoxidation and the factors that control it. *iii*) How does the product control evolve with increasing energy of the photolysis photons? In particular, is there a loss of product specificity as the photolysis wavelength is tuned through the NO_2 dissociation limit? *iv*) How does the chemistry of collisional pairs in a matrix compare with the chemistry of the same reactants in solution or gas phase?

Investigation of the (Z)-but-2-ene + NO_2 reaction by a similar series of wavelength-dependent photolysis experiments allowed us to address the first two points. In very

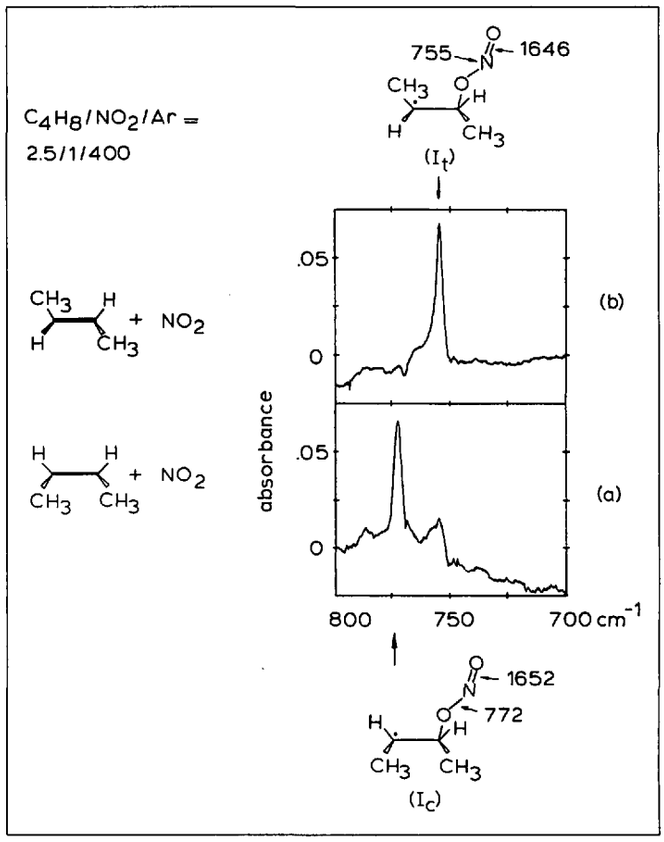

Fig. 4. *IR absorptions of butyl-nitrite radical conformers. a*) Absorbance growth in the ν(N–O) region upon 590 nm photolysis of a matrix (*E*)-but-2-ene/NO_2/Ar = 2.5/1/400. *b*) Growth upon irradiation of a matrix (*Z*)-but-2-ene/NO_2/Ar = 2.5/1/400 at 590 nm. The small negative feature at 771 cm^{-1} in both spectra is due to N_2O_3 [3].

dilute (*Z*)-but-2-ene/NO_2/Ar matrices, the red-light-induced reaction of (*Z*)-but-2-ene · NO_2 pairs gave exclusively *cis*-2,3-epoxybutane as final oxidation product [6]. Again, a butyl-nitrite radical was concurrently formed, but its IR absorptions did not coincide with those of the (*E*)-but-2-ene + NO_2 reaction. For instance, the N–O bond stretching region (*Fig. 4*, butene/NO_2/Ar = 2.5/1/400) shows nitrite-radical absorption at 772 cm^{-1} for the product of (*Z*)-but-2-ene + NO_2 (labelled I_c), while the corresponding (*E*)-butene + NO_2 product band is found at 755 cm^{-1} (species labelled I_t). However, we found that warmup from 12 to 22 K of a matrix containing I_c leads to complete loss of the I_c bands and concurrent growth of I_t absorptions. This indicates that I_c and I_t are stereoisomers, and that I_c is the less stable of the two. IR spectral analysis, together with this clue about relative energies enabled us to assign I_t to a butyl-nitrite radical with *anti*-conformation about the central C–C bond with respect to the CH_3 groups, and I_c to the corresponding *syn*-conformer [6] (*Fig. 4*; conformation about the N–O bond is *trans* for both I_t and I_c, while the conformation with respect to the C–O bond remains undetermined). Hence, the butyl-nitrite-radical conformer observed in each case is the one expected, if configuration about the former C=C bond is retained. The fact that the epoxide product was also formed diastereospecifically is consistent with, but does not require that, the paths leading to the two products share a common step. The latter was established, however, by observation of a correlation of the configuration of butyl-nitrite radical and epoxide under conditions where partial stereochemical scrambling did occur. This was observed when conducting the (*Z*)-but-2-ene + NO_2 reaction at high reactant concentration. For example, upon increase of the reactant concentration from (*Z*)-but-2-ene/NO_2/Ar = 2.5/1/400 to 2.5/1/100, the *syn*/*anti* (*cis*/*trans*) ratios of epoxide and nitrite radical decreased both by the same factor, namely from 6 to 1 (interestingly, no stereochemical scrambling occurred ever in the (*E*)-but-2-ene + NO_2 reaction at any concentration). This parallel behavior implies that the butyl-nitrite radical and the epoxide have a common transient precursor whose configuration dictates that of both products.

The sole transient precursor which is consistent with our observations in all hydrocarbon + NO_2 photoreactions studied so far is an oxirane biradical, shown in *Fig. 1*. Direct O-atom transfer to the C=C is in accord with the nature of vibronic states prepared upon excitation of NO_2 with long-wavelength visible quanta. The excited $^2B_2$ state which gives NO_2 its oscillator strength in the VIS and NIR is strongly coupled with high vibrational levels of the $^2A_1$ ground electronic state according to extensive high-resolution gas-phase studies [4]. In fact, this mixing of $^2B_2$ and $^2A_1$ states is so strong that the photo-excited NO_2 is best described as a highly vibronically excited species with predominant electronic ground-state character. Since a large fraction ($^2/_3$) of the NO_2 vibrational modes are stretching modes, high-vibrational-overtone excitation by VIS light (16400 cm^{-1} upon absorption of a 610 nm photon) results in motion of the NO_2 · alkene collisional pair along an asymmetric N–O···C large amplitude stretching coordinate that corresponds approximately to the reaction coordinate for O-atom transfer (the O···C=C distance contracts as the N–O bond expands because the C=C group is spacially fixed). The oxirane biradical so produced is stabilized by two processes that compete on an ultrashort timescale, namely ring closure to form epoxide, and radical combination with concurrently generated NO cage neighbor to give a butyl-nitrite radical (*Fig. 1*). Thus, the observed butyl nitrite radical constitutes a chemically trapped transient oxirane biradical. The interesting point is that the transient biradical is trapped in its nascent conformation, which means that, by determining the conformation of the spectroscopically observed nitrite radical, we are able to probe for the first time the structure of the transient biradical that controls the configuration of the epoxide.

Apart from the chemical trapping of transients, it is the high degree of stereochemical integrity of the reaction that caught our interest. This is, no doubt, a direct result of the long wavelength of the photons used to excite the reaction. If we take the *ab initio* work on ethylene oxirane biradical as a guide [7][8], we find that an alkene · NO_2 pair excited at 600 nm has just enough energy to access the $^1D(\sigma\sigma)$ ground electronic state of the biradical, but not any of the excited states. In this biradical state, the singly occupied p orbitals on C and O lie both in the CCO plane (*Fig. 1*), *i.e.* are in perfect alignment for the ring to close. In fact, this state lies on the electronic ground-state surface of the epoxide. This is probably the main factor responsible for the observed high stereochemical integrity, since such adiabatic ring closure is expected to be sufficiently fast (ps) to compete successfully with scrambling about the central C–C bond (the partial scrambling observed in the (*Z*)-but-2-ene epoxidation under certain matrix conditions, and by contrast, its complete absence in the (*E*)-but-2-ene + NO_2 case can be rationalized on the basis of more potential-energy release in the form of internal rotational energy upon $sp^2 \rightarrow sp^3$ rehybridization in the (*Z*)-case as the O-atom approaches to the C=C bond) [6]. A special benefit then of the use of long-wavelength photons is exclusive access to the lowest electronic state of the primary transient photoproduct, which for the reaction discussed here leads adiabatically to the final product in its ground state. As will be illustrated for cycloalkene + NO_2 reactions in *2.1.2*, use of shorter wavelength photons (λ<400 nm) results in loss of product control as transient oxirane biradicals acquire excess internal kinetic and/or electronic energy that opens up rearrangement processes not accessible upon photolysis at long VIS wavelengths. Of course, generation of primary photoproduct with the least amount of excess kinetic and electronic energy hinges not only on the energy of the exciting photon, but also on the overall free energy change of the atom-transfer reaction. In this respect, NO_2 is an oxidant that is particularly well tuned to the use of long-wavelength VIS photons for controlled chemistry.

Study of O-atom transfer of vibronically excited NO_2 · ethylene pairs gave us an opportunity to probe in more detail the dynamics of this mild hydrocarbon photo-oxidation process. The potential energy profile of the C_2H_4 + NO_2 system is very similar to that of the but-2-ene + NO_2 reaction shown in *Fig. 1*, except that the ^1D ethylene oxirane

Scheme 1

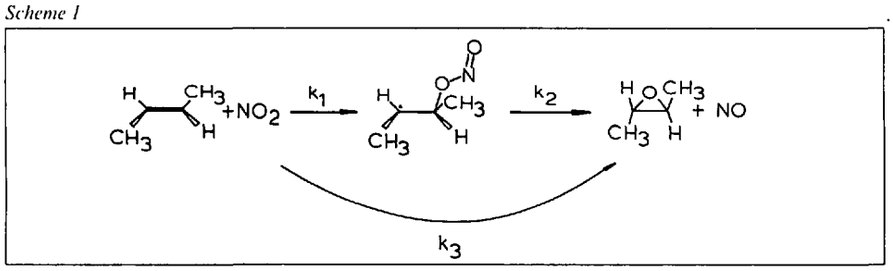

Scheme 2

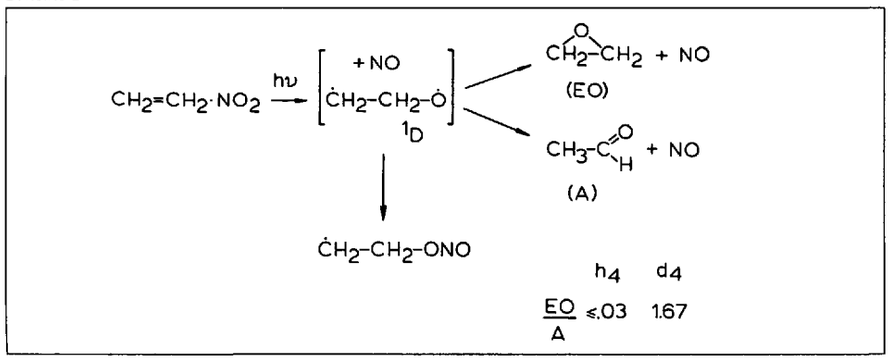

biradical has a low-barrier intramolecular 1,2-H migration path available (to give acetaldeyde) in addition to the ring closure channel [7][9] (*Scheme 2*). In fact, we found that excitation of $C_2H_4 \cdot NO_2$ pairs in solid Ar at 575 nm (photolysis threshold) and shorter yellow, green, and blue wavelengths produced exclusively aldehyde along with the expected ethyl-nitrite radical [10] (intramolecular 1,2-H migration at the expense of epoxide formation has been found exclusively for olefins with terminal C=C bonds, *e.g.* also in the case of isobutylene [11]). Ethylene oxide was also detected, but quantitative kinetic analysis of product absorbance growth curves showed that it originated exclusively from photodissociation of accumulated ethyl nitrite radical [10]. Taking into account our absorbance detection limit, the upper limit of the ethylene oxide/acetaldehyde (EO/A) product ratio upon $C_2H_4 \cdot NO_2$ photolysis is estimated at 0.03. In contrast, the EO/A branching ratio of the perdeuterated products derived from kinetic analysis of $C_2D_4 + NO_2$ product growth curves was much larger, namely 1.7 [12]. This shift towards ring closure at the expense of acetaldehyde formation upon D substitution implies that aldehyde and epoxide have a common transient precursor, consistent with the proposed formation of oxirane biradical. The lifetime of the biradical must be extremely short (ps) as no stereochemical scrambling by rotation about the C–C bond was observed in chemically trapped ĊHD–CHD–Ȯ despite a very low barrier, estimated at less than 1 kcal mol^{-1} [8]. This is based on observation of mutually exclusive ĊHD–CHD–ONO IR spectra upon yellow light induced reaction of (*Z*)-CHD=CHD and (*E*)-CHD=CHD with NO_2 (*Scheme 3*) [10]. Similar to the but-2-ene + NO_2 case, we noticed a sharp, 13-fold increase of the quantum efficiency to ethylene + NO_2 reaction with photolysis photon energy in the narrow, 5-kcal range between 575 and 514 nm. Such a steep increase in the vicinity of the 16000-cm^{-1} barrier estimated for oxirane biradical formation is typical for statistical (RRK) behavior, as we would expect it for reactions of highly vibrationally excited NO_2 [13].

2.1.2. *Cyclohexene + NO_2*

A unique aspect of these mild photo-oxidations of olefins in a solid matrix is the chemical trapping of oxirane biradical transients in their nascent conformational distribution. This gives us an opportunity to explore not only the regiochemical, but also the detailed stereochemical path of olefin oxidations. We found that O-atom transfer to isobutylene is regioselective, occurring exclusively to the terminal C-atom [11]. This is perhaps not too surprising, as it constitutes the sterically more accessible C-atom, and leads to the oxirane biradical presumed to be thermodynamically more stable. A subtle, stereochemical question is raised by cycloalkene epoxidations. 600-nm photolysis of cyclohexene · NO_2 collisional pairs, *e.g.*, gave cyclohexene oxide as sole final oxidation product (*Scheme 4*) [14]. While comparison of the (half-chair) structures of reactants and products gives no clue as to the branching between the two possible diastereoisomeric O-atom transfer paths (attack on one or the other side of the C=C bond), IR spectra of cyclohexyl-nitrite radical, if formed, would allow us to address this problem. Two distinct sets of nitrite-radical IR absorptions grew in upon red-light photolysis of cyclohexene · NO_2 pairs as indicated by intense *doublets* in the υ(N=O) and υ(N–O) regions displayed in *Fig. 5*. The spectra of *Fig. 5* actually show the depletion of the trapped species by wavelength selective photodissociation at 545 nm (spectrum a) and 514/488 nm (spectrum b) after initial accumulation of nitrite radical by 590-nm irradiation of cyclohexene · NO_2 pairs.

Comparison of *Fig. 5a* and *b* clearly establishes the presence of two distinctly different nitrite radicals, namely by the preferential depletion of one (1644/756 cm^{-1}, labelled I_2) over the other (1655/769 cm^{-1}, labelled I_1) upon 545-nm photolysis. On the basis of these selective photodissociation experiments, all 16 IR bands assigned to the two nitrite radical species could be separated into these two groups. Photoproducts of both I_1 and I_2 were cyclohexene oxide and NO, which confirmed that the two species were cyclohexyl-nitrite radical conformers.

^{15}N and ^{18}O isotopic IR data allowed us to establish I_1 as a cyclohexyl-nitrite radical with an equatorial, I_2 as one with an axial CO group [14]. While IR spectra did not furnish any clue as to the conformation of the ring (chair or twist-boat), the possibility that I_1 or I_2 has unstable twist-boat conformation could virtually be ruled out as we did not observe any $I_1 \leftarrow I_2$ interconversion at matrix temperatures well above the estimated twist-boat to chair isomerization barrier [14]. The latter was estimated to lie around 0.7 kcal mol^{-1}, based on approximation of the cyclohexene oxirane biradical potential by that of cyclohexyl radical as shown in *Fig. 6*. Hence, our results indicate that both observed cyclohexyl-nitrite radicals have chair conformation, and that I_1 has the CO group in equatorial, I_2 in axial position. As indicated in *Fig. 6* this implies that I_1 is chemically trapped CH-e oxirane biradical, while I_2 is a biradical trapped in the

Scheme 3

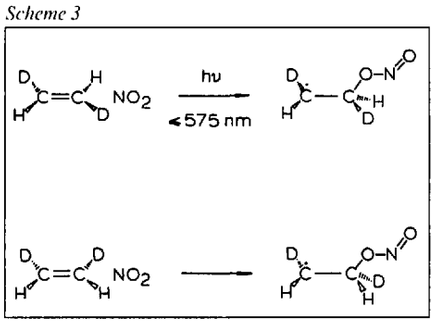

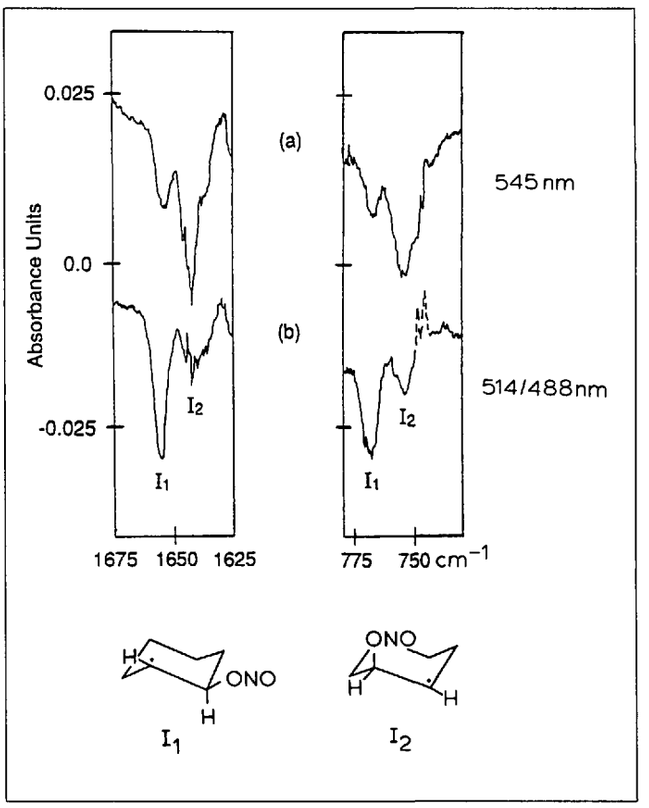

Fig. 5. *Wavelength-selective photodissociation of cyclohexyl nitrite radical conformers. a*) Decrease of N=O and N–O stretching absorptions upon 30-min photolysis at 545 nm (150 mWcm^{-2}) following accumulation of cyclohexyl-nitrite radical by prolonged irradiation of a matrix cyclohexene/NO_2/Ar = 2.5/1/100 at 590 nm. *b*) Depletion of the same bands upon further photolysis at 514/488 nm (100 mWcm^{-2}) for 5 min.

Scheme 4

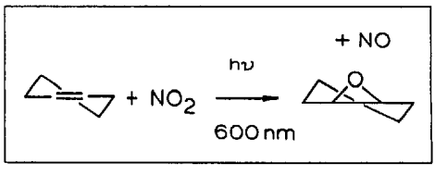

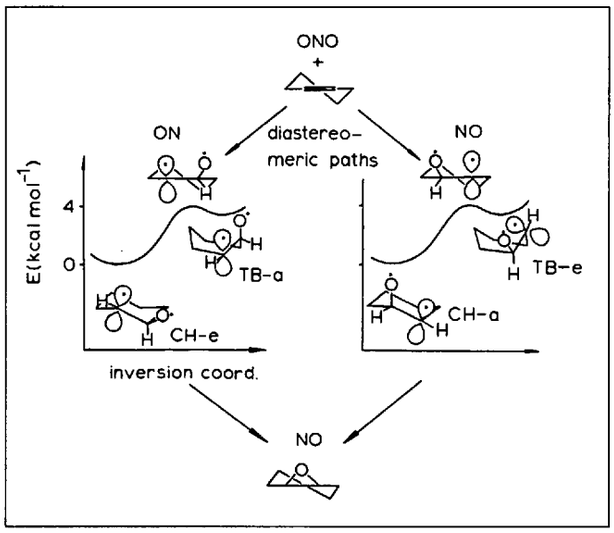

Fig. 6. *Stereochemistry of cyclohexene + NO_2 O-atom transfer path.* Ring-inversion potential of cyclohexene oxirane biradical is approximated by that of cyclohexyl radical [15].

CH-a conformation. This assignment is further supported by the observed difference in the photodissociation efficiency of I_1 and I_2 [14].

If our estimate of the twist-boat to chair interconversion barrier is correct, any twist-boat (TB) cyclohexene oxirane biradical, if it were formed, is expected to be trapped as TB nitrite radical. The only way by which TB cyclohexyl nitrite radical could have gone undetected is by thermal interconversion to the chair form prior to recording of an IR spectrum (timescale of min). However, in a 12 K environment this would imply an isomerization barrier substantially below its estimated value of 0.7 kcal mol^{-1} [16]. Therefore, it is most likely that CH-e and CH-a are the nascent conformations of cyclohexene oxirane biradical. Hence, both diastereoisomeric O-atom transfer paths are pursued, each leading specifically to one particular oxirane biradical stereoisomer. A fraction of these is trapped as cyclohexyl-nitrite radical (I_1 or I_2) by combination with NO cage neighbor, while the rest undergoes ring closure to yield cyclohexene oxide. The apparent lack of formation of TB oxirane biradical suggests that the initial half-chair nuclear configuration of the ring relaxes towards a chair form as the attacked C-atom undergoes $sp^2 \rightarrow sp^3$ rehybridization regardless to which side of the C=C bond the O-atom is transferred [17].

To address the question posed in *2.1.1* as to the extent to which the observed high product specificity of these oxidations may be a consequence of excitation of alkene · NO_2 pairs below the NO_2 dissociation threshold, cyclohexene and cyclopentene/NO_2/Ar matrices were irradiated with light at wavelengths shorter than the 398 nm dissociation limit. Experiments were conducted with the 355 nm output of a pulsed Nd:YAG laser or the 351–364 nm emission lines of a cw Ar ion laser, leading to results that were independent of photolysis source. As can be seen from IR absorbance growth curves of cyclohexene + NO_2 reaction products shown in *Fig. 7*, loss of product control is indicated by the appearance of cyclohexanone and cyclohex-2-en-1-ol along with cyclohexene oxide already observed upon photolysis at long wavelengths [14]. A similar set of new products was obtained upon 355 nm excitation of the cyclopentene + NO_2 reaction. An obvious possibility for loss of product specificity upon irradiation at energies above the NO_2 dissociation limit is predissociation of the reactant to $O(^3P)$ ground-state atoms and NO (*Fig. 7*, insert; the absorption cross section in the 350-nm region is due to the bound $^2B_2$ state). Thermal addition of O-atoms so produced to the C=C bond may lead to products different from those of large amplitude O-atom transfer of alkene · NO_2 pairs. The latter path is accessible, at least in principle, at any photolysis photon energy above the 610 nm reaction threshold irrespective of whether excitation occurs above or below the NO_2 dissociation limit. In addition, loss of product specificity at short photolysis wavelengths may also occur along the large amplitude path. The reason is that transient oxirane biradicals emerging from large amplitude O-atom transfer induced at 350 nm carry substantially more excess internal energy than those formed by long-wavelength VIS light, hence have an increased propensity to rearrange or fragment. The competition between predissociation of NO_2 and coupling into the asymmetric N–O···C large amplitude stretching coordinate is expected to depend to a certain degree on the geometry of the collisional pairs.

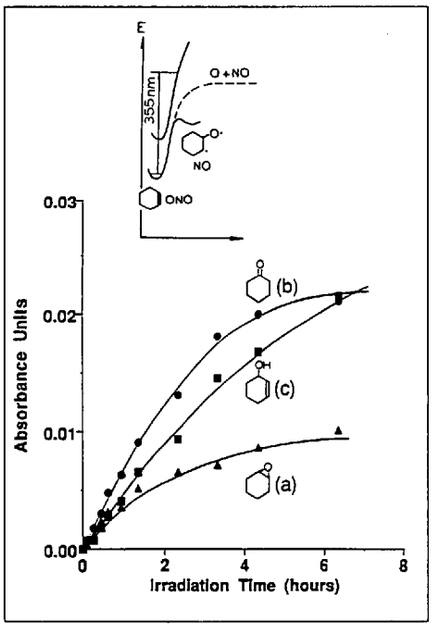

Fig. 7 *Absorbance growth kinetics upon irradiation of a matrix cyclohexene/NO_2/Ar = 2.5/1/200 at 355 nm* (8 $mWcm^{-2}$). *a*) cyclohexene oxide (968 cm^{-1}), *b*) cyclohexanone (1723 cm^{-1}), *c*) cyclohex-2-en-1-ol (1067 cm^{-1}). Insert shows potential-energy diagram of cyclohexene + NO_2 reaction.

Comparison of the shapes of the product absorbance growth curves of *Fig. 7* gives a clue as to the origin of the new products. The cyclohexanone growth behavior is the same as that of cyclohexene oxide, but the growth kinetics of cyclohexenol is distinctly different. This strongly suggests that cyclohexanone originates from the same reactant reservoir as cyclohexene oxide, *i.e.* the pool of cyclohexene · NO_2 collisional pairs that already undergo large amplitude O-atom transfer upon excitation below the NO_2 dissociation limit. This leads us to conclude that upon 355-nm photolysis, epoxide and ketone (at least a fraction of it, see discussion in [14]) are produced *via* a common ground-state ^1D oxirane biradical along the large amplitude O-atom transfer path, consistent with the fact that the cyclic ketones are 1,2-H shift products that can only originate from a singlet, but not from a triplet oxirane biradical [7][9]. It manifests the adverse impact, in terms of product control, of excess internal energy in the primary transient photoproduct, which is a direct result of the short-wavelength photons used to initiate the reaction.

On the other hand, the reactant reservoir that yields cyclohexenol must be substantially larger than the pool giving rise to epoxide and ketone according to the growth curves of *Fig. 7*. The only reactant that absorbs at 355 nm and whose reservoir exceeds that of alkene · NO_2 collisional pairs is isolated NO_2. Hence, cyclohexenol is produced by dissociation of NO_2 to $O(^3P)$ and NO, followed by combination of O-atoms with cyclohexene. The reactant reservoir presumably involves NO_2 separated from a hydrocarbon molecule by one or several layers of Ar host atoms, as well as alkene · NO_2 cage pairs with unfavorable geometry to react along the large amplitude O-atom transfer coordinate. Although conservation of spin requires that the $O(^3P)$+cyclohexene step leads to triplet-excited oxirane biradical initially, no conclusion can be drawn as to the biradical state in which subsequent 1,4-H migration to cyclohexenol takes place. In any case, the loss of product control upon excitation of alkene · NO_2 collisional pairs above the dissociation limit is in accord with the multiple products observed in the case of $O(^3P)$+alkene reactions in cryogenic solids [18].

Despite the loss of product control upon photolysis at energies above the dissociation limit, it is interesting that there remains a substantial propensity for cycloalkene · NO_2 sustained collisional pairs to couple into the large amplitude O-atom transfer path rather than to proceed along the dissociation-addition path. In fact, there is a growing number of reports of bimolecular photochemical reactions of weak complexes in cryogenic matrices and in molecular beams that also point to preferred coupling into large amplitude atom transfer coordinates. For example, recent work by *Andrews* and coworkers suggests that O_3 engaged in weakly bound complexes with PH_3, PCl_3, and other group V halides in solid rare-gas matrices undergoes O-atom transfer without dissociating to $O(^3P)+O_2$ when excited to the $^1B_1$ state by red light [19]. UV-light-induced chemistry of acetylene · HI complexes in solid Kr by *Abrash* and *Pimentel* constitutes an extreme case in that photo-excitation promotes HI directly onto a dissociative surface [20]. Yet there is evidence that, even in this situation, the reaction path does not involve formation of H-atoms, but instead direct coupling of the excited HI · acetylene complex into C_2H_3 + I product states *via* a large amplitude I–H···C_2 coordinate. Access to this reaction path is attributed to the special T-shaped geometry of the complex formed by the reactants. Such precursor geometry limited H-atom transfer reactions in which no free H-atoms are formed along the reaction path have previously been recognized by *Wittig* and coworkers upon photo-excitation of weak complexes (*e.g.* CO_2 · HBr) in molecular beams [21]. The finding that large amplitude H-atoms transfer reactions are also observed in the absence of a matrix cage clearly shows that the dynamics of the initial reaction step of the excited pair is not dictated by the solid matrix environment. The only apparent function of the matrix cage in the initial stage of the reaction is to sustain the collisions (or weak complexes).

2.1.3. *Oxidation of Allene and Alkynes*

The high product specificity of olefin oxidations by long-wavelength VIS light photolysis of NO_2 · alkene collisional pairs made it extremely interesting to explore the same approach for controlled allene and alkyne oxidation. Particularly intriguing was the prospect of mapping the detailed stereochemical path of cumulene and triple bond oxidations by chemical trapping of transient biradicals. Transients postulated for these reactions[22][23][24] have eluded observation thus far.

We observed the reaction threshold of CH_2=C=CH_2 · NO_2 collisional pairs at 585 nm [24]. A nitrite radical grew in whose NO photo-elimation products formed upon subsequent irradiation at 488 nm were allene oxide and cyclopropanone (*Scheme 5*). The latter can only originate from photodissociation of a nitrite radical with the ONO group

Scheme 5

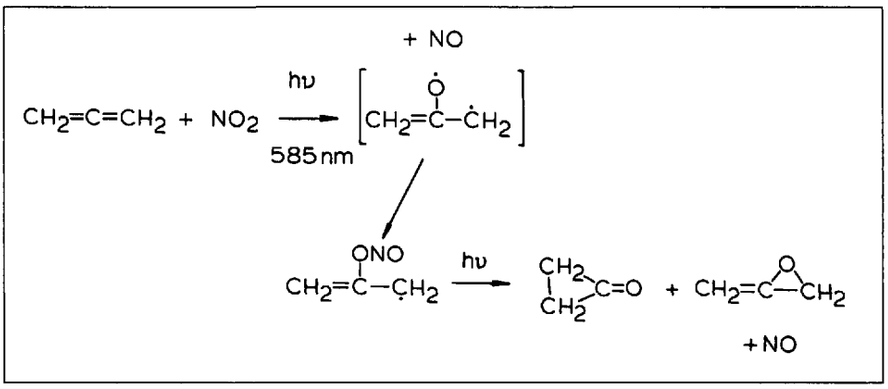

at the central, but not the terminal C-atom. Moreover, only a single nitrite-radical isomer was observed, hence transient biradical with O at the central position is formed exclusively. Obviously, O-atom transfer occurs only to the central C-atom of allene, leading to the thermodynamically preferred, allyl-stabilized biradical rather than the biradical corresponding to attack at the terminal position.

Interestingly, O-atom transfer from NO_2 to a C≡C bond does not give a nitrite radical, but an iminoxy radical instead. For example, when photolysing dimethylacetylene · NO_2 pairs at 600 nm four isomeric acetyl methyl iminoxy radicals were formed (*Fig. 8*) [24]. Dimethylketene and NO are produced concurrently in a direct, single photon process as indicated by growth of the characteristic ketene CO stretching absorption at 2130 cm^{-1} with its 28 cm^{-1} ^{18}O shift. IR spectroscopic evidence for iminoxy radical is primarily based on two groups of bands, 1716–1707 cm^{-1} and 1600–1545 cm^{-1} that exhibit ^{18}O and ^{15}N frequency shifts characteristic for υ(C=O) and υ(C=N) modes, respectively. As can be seen from the spectrum of *Fig. 8*, most absorptions of the iminoxy radical are split into several bands. Wavelength-dependent growth behavior and selective photo-isomerization experiments with green light allowed us to establish four separate spectra which are attributed to s-*cis*- and s-*trans*-conformers with respect to the central CC bond, and *syn*- and *anti*-stereoisomers with respect to the position of the iminoxy O-atom.

Aside from the tight control of long-wavelength-light-induced allene and acetylene + NO_2 photochemistry in terms of final oxidation products (ketenes were exclusive final oxidation products of HC≡CH and CH_3C≡CH oxidations as well) [25], most significant is the observation of iminoxy radicals, but no nitrite radicals, in the case of reaction of C≡C bonds. It has long been speculated that oxirenes (–C=C–O) are transients formed upon oxidation of C≡C bonds [23], hence trapping of this species, or chemical trapping of its –Ċ–C–Ȯ biradical precursor state in the form of a nitrite radical could have been expected. The iminoxy radical observed instead correponds to NO trapped ketocarbene biradical (*Fig. 8*). This indicates that O-atom transfer to a C≡C bond results in direct formation of the biradical in

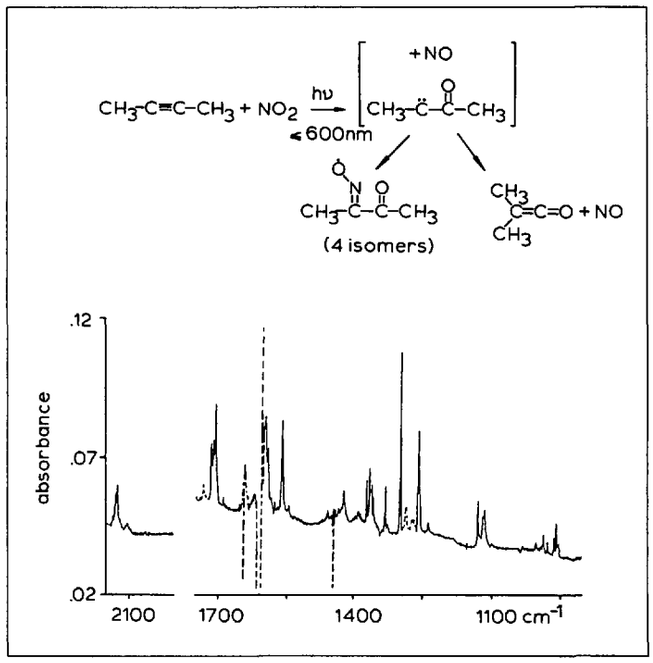

Fig. 8. *IR product growth upon 85-min irradiation of a matrix dimethylacetylene/NO_2/Ar = 2.5/1/200 at 585 nm.* All solid bands originate from iminoxy-radical isomers, except for those due to dimethylketene around 2100 cm^{-1}. Dashed absorptions are due to reactants or N_xO_y species.

a ketocarbene state, and that no transient oxirene is formed (the fact that an electronically excited $CH_2C(\dot{O})\dot{C}H_2$ transient biradical is trapped by NO in the allene + NO_2 case suggests that any transient biradical state preceding ketocarbene in the alkyne + NO_2 case, if it were formed, would most likely be trapped by NO) [24]. Branching between ketene and iminoxy radical is dictated by competition between *Wolff* rearrangement [26] of transient ketocarbene and combination with NO cage neighbor.

A more general conclusion regarding observation of completely different trapped intermediates upon alkyne and alkene/allene photo-oxidation (iminoxy *vs.* nitrite radical) is that it confirms formation of a transient biradical by direct O-atom transfer as the key elementary step of vibronically induced reaction of NO_2 · hydrocarbon pairs. Interestingly, thermal reaction of unsaturated hydrocarbons in gas phase or solution leads to nitroalkyl radicals, *i.e.* to C–N bond formation [27] rather than O-atom transfer. This difference between matrix and fluid phase alkene+NO_2 chemistry is surprising in view of the fact that NO_2 excited by low-energy VIS photons has predominantly the character of a highly vibrationally excited electronic ground-state species, hence would be expected to have chemistry similar to that of thermally excited $NO_2(^2A_1)$. As discussed in detail elsewhere [10], the different chemistry in fluid phase and solid matrix manifests the preferred access of the vibronically excited collisional pair to a large amplitude O-atom transfer coordinate while ignoring a lower barrier translational (in the solid: *van der Waals*) coordinate that would lead to C–N bond formation by NO_2 addition.

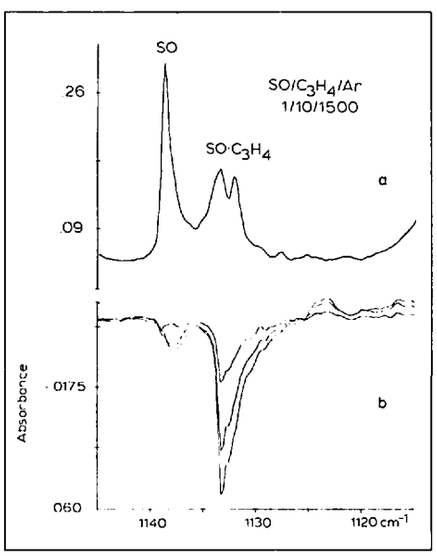

Fig. 9. *SO stretching absorption in a matrix SO/allene/Ar = 1/10/1500. a*) Spectrum before photolysis, showing distinct bands for isolated SO and weak SO · allene complexes. *b*) IR difference spectra upon 3 consecutive NIR photolysis periods by filtered tungsten source light in the region 3000–12000 cm^{-1}. Reaction was also observed when limiting photolysis light to the 5700–5900 cm^{-1} range. Depletion occurs where SO · allene complexes absorb. The small loss of absorbance at the low frequency side of the 1138 cm^{-1} band of isolated SO is due to photon induced local diffusion.

2.2. *Reactions of Singlet Excited SO and O_2*

The hydrocarbon + NO_2 reactions demonstrate that unique chemistry can be accomplished by single-photon excitation of reactants that are held together in a sustained collision in a solid matrix cage. The high product specificity of these long-wavelength-light-induced oxidations is the result of exclusive access to products that are formed by large amplitude O-atom transfer, and the fact that primary photoproducts emerge with only a modest excess internal energy. However, controlled chemistry of collisional pairs with long-wavelength photons is by no means limited to large-amplitude atom-transfer reactions. As the following examples show, there are efficient cycloaddition reactions of metastable electronically excited molecules that can be initiated with light deep in the NIR.

2.2.1. *Cycloaddition Reactions of Singlet SO*

Sulfur monoxide has two very low, strongly bound singlet-excited states, namely the $a^1\Delta$ state with a minimum at 5800 cm^{-1} (16.7 kcal mol^{-1}), and the $b^1\Sigma^+$ state with its minimum at 10500 cm^{-1} (30 kcal mol^{-1}). These states are metastable with respect to decay to the triplet ground state ($^3\Sigma^-$) [28]. While reports on thermal solution and gas-phase reactions of SO confirm the radical-like character of its ground-state chemistry [29], reactions of singlet excited SO have remained completely unexplored. Yet on the basis of simple molecular-orbital and spin considerations, one would expect the chemistry of singlet SO to be distinctly different from that of the ground state species [30].

We have explored singlet SO chemistry by direct photo-excitation of SO · allene and SO · acetylene pairs in solid Ar [31]. SO was generated during deposition of the matrix by pyrolysis of a convenient precursor, ethylene episulfoxide, in the vacuum deposition line. In contrast to the hydrocarbon + NO_2 reactions, where we had no indication of complex formation, SO · hydrocarbon cage neighbors form weak complexes as signaled by distinct SO IR absorptions that are shifted to lower frequency relative to the isolated SO band by several cm^{-1}. This is displayed in *Fig. 9* (upper part) for the SO · allene system. The sequence of IR difference spectra shown in the lower part of *Fig. 9* indicate that NIR irradiation at energies as low as 5800 cm^{-1} leads to chemical reaction. Depletion is observed mainly where SO · allene pairs absorb, which confirms that reaction proceeds in the absence of bulk diffusion.

Product of the SO + allene reaction is allene episulfoxide, synthesized by this method for the first time (*Scheme 6*). The structure of the product was in essence established by the very intense S=O stretching band around 1100 cm^{-1}, and an intense absorption at 916 cm^{-1} which is characteristic for the out-of-plane wagging mode of an olefinic CH_2

Scheme 6

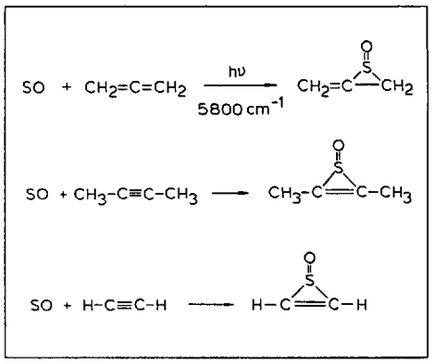

group [31]. Allene episulfoxide is indeed the product which one would expect from spin conserved, orbital allowed [1+2] cycloaddition of singlet SO across the C=C [32]. This signals an electronic-state-specific reaction on the excited singlet surface, as no [1+2] cycloaddition products have been reported for triplet-ground-state SO reactions [29]. Since reaction between SO and allene occurs upon selective excitation of SO to the vibrationless level of the $^1\Delta$ state even in a 12 K environment, the barrier on the singlet reaction surface must be very small (well below 1 kcal mol^{-1} assuming that tunneling plays no role). Such adiabatic reaction of vibrationally relaxed collisional pairs on an excited electronic surface is distinctly different from the NO_2 + hydrocarbon case where high vibrational reactant excitation was found to be essential (the large-amplitude nuclear motion that brings about cycloaddition of SO ($^1\Delta$) to allene is a low frequency *van der Waals* motion of the weak complex). As shown in *Scheme 6*, similar NIR induced [1+2] cycloaddition on the singlet surface has also been accomplished in the case of C≡C bonds, leading to new heterocyclopropene episulfoxides [31].

This first singlet SO chemistry demonstrates that long-wavelength NIR photons offer a way to accomplish new chemical synthesis. The observed product specificity has its origin in part in the chemical properties of the excited, metastable electronic state of the reactant. A crucial additional factor is again the modest excess energy with which products emerge from reaction due to the long-wavelength quanta used to excite the reactants. It allows stabilization of these unusual three-membered ring molecules which otherwise might fragment or rearrange prior to deactivation by the matrix environment.

2.2.2. *Cycloadditions of Singlet O_2*

Like SO, molecular oxygen has two metastable excited states at energies deep in the NIR, namely the $^1\Delta_g$ state with its minimum around 8000 cm^{-1} and the $^1\Sigma_g$+ state at 13000 cm^{-1} [33]. As shown in the insert of *Fig. 10*, these states are situated well below the 41000 cm^{-1} dissociation limit of the molecule. O_2 in the $^1\Delta$ state is a particularly attractive reactant for chemistry with NIR photons because of its unusually long life-

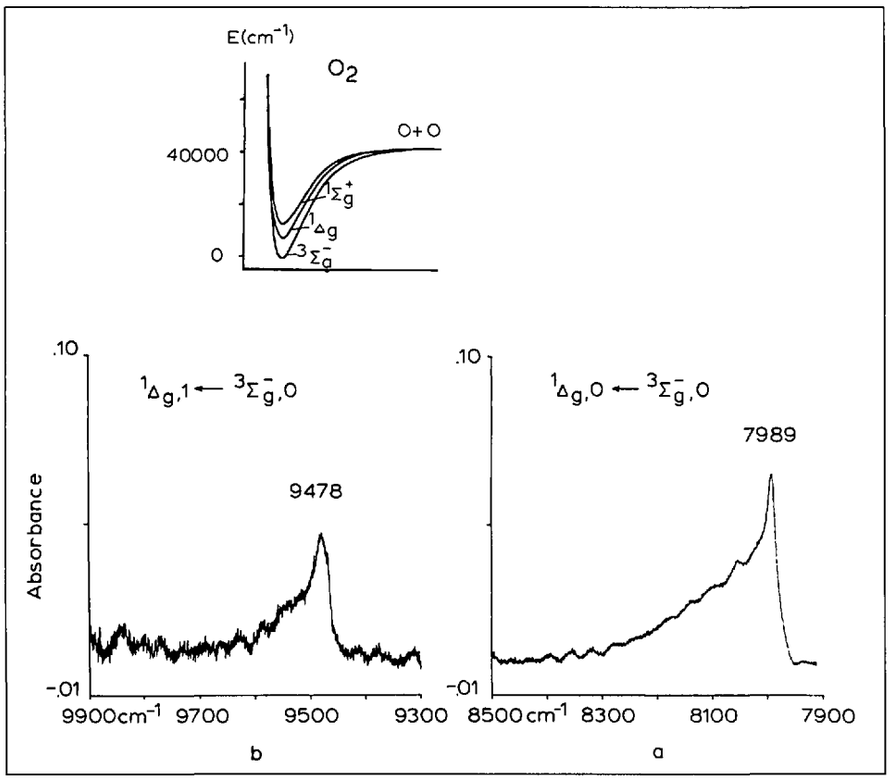

Fig. *10. NIR absorption spectra of the (0,0)* (spectrum a) *and (1,0)* (spectrum b) *transitions of singlet delta O_2 in solid α-oxygen at 12 K.* Insert shows potential curves of ground and lowest excited singlet states of O_2 [33].

time (minutes in solid matrices [34], tens of microseconds to several milliseconds in room-temperature solution [35]) and its strong electrophilic character. These properties make $O_2(^1\Delta)$ a key intermediate in many reactions, *e.g.* sensitized photo-oxygenations. Indeed, the chemistry of singlet O_2 has been an active research field for almost three decades now [36].

One type of singlet-O_2 reaction of special interest regarding the use of NIR photons is *Diels-Alder* addition to conjugated dienes to form endoperoxides (*Scheme 7*). Several aromatic endoperoxides are known to release O_2 in its excited singlet state upon cycloreversion, hence are a form of chemically stored singlet excited O_2 molecules. If it were possible to directly convert retrieved $O_2(^1\Delta)$ electronic energy into electricity, $O_2(^1\Delta)$+diene $\rightleftarrows$ endoperoxide systems might serve as a model for temporary chemical storage of NIR photons and their efficient conversion into useful energy. While experiments to explore this concept will be primarily the theme of *Sect. 3* below, we will mention here briefly selective vibronically induced reactions of diene · O_2 collisional pairs in solid O_2 and in Ar matrices that probe the efficiency of NIR light of various wavelengths in promoting chemical storage of $O_2(^1\Delta)$, and that serve to elucidate the dynamics of the reaction on the singlet hypersurface. Such insight was not available from previous VIS light photosensitized singlet O_2 + diene reactions in solution [35][36].

NIR *Fourier*-transform absorption spectroscopy was employed to monitor the precise frequency of the $v = 0$ and $v = 1$ level of the $^1\Delta$ state in solid α-O_2 (*Fig. 10*) [37]. Although extremely weak in the gas phase because of their rigorous spin- and orbital-forbidden nature in electric dipole absorption, these bands are enhanced in solid O_2 because of the interaction with neighboring O_2 molecules [38]. Indeed, selective vibronic excitation of either transition with narrow band pass filtered tungsten source light in solid O_2 or solid Ar induced addition of O_2 to furan and Me-substituted furans to yield the corresponding endoperoxides [37]. Structures of these products were established by IR analysis based on ^{18}O data. As in the case of SO, the higher energy $^1\Sigma_g^+ \leftarrow {}^3\Sigma_g^-$ progression was too weak for detection by conventional NIR spectroscopy. However, monitoring the IR product absorbance growth while tuning the cw dye photolysis laser through the spectral region where these vibronic transitions were expected to absorb (13000–15000 cm^{-1}) allowed us to determine their precise position (laser-reaction-excitation spectroscopy). Quantum efficiencies turned out to be very high even upon excitation of the ground vibrational level of the $^1\Delta_g$ state at 8000 cm^{-1}: $\phi = 1.0$ for dimethylfuran + O_2, 0.64 for methylfuran + O_2, and 0.38 for furan + O_2, with virtually no differences among the various $^1\Delta_g$ and $^1\Sigma_g^+$ vibronic states [37]. This is consistent with reaction of vibrationally relaxed $O_2(^1\Delta)$ · furan pairs on the singlet hypersurface irrespective of which $^1\Delta_g$ or $^1\Sigma_g^+$ vibronic state was prepared initially by photo-excitation, similar to the case of singlet SO cycloaddition reactions.

It is important to note that the observed high quantum efficiency to reaction coupled with low absorption cross section of the reactant makes a solid matrix an ideal environment for conducting controlled chemical synthesis with NIR light. In fact, low extinction coefficients are typical for molecules with low-lying states in the NIR, and a solid matrix offers a medium for achieving the high density of reactant pairs required to make maximum use of the incident photon flux.

2.3. *Low-Energy Paths of other Reactions of O_2*

Laser-reaction-excitation spectroscopy of collisional pairs, which already allowed us to uncover the very weak $^1\Sigma^+ \leftarrow {}^3\Sigma^-$ progressions of SO and O_2, became most useful

Scheme 7

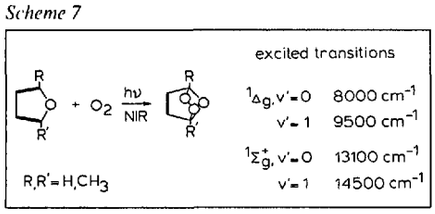

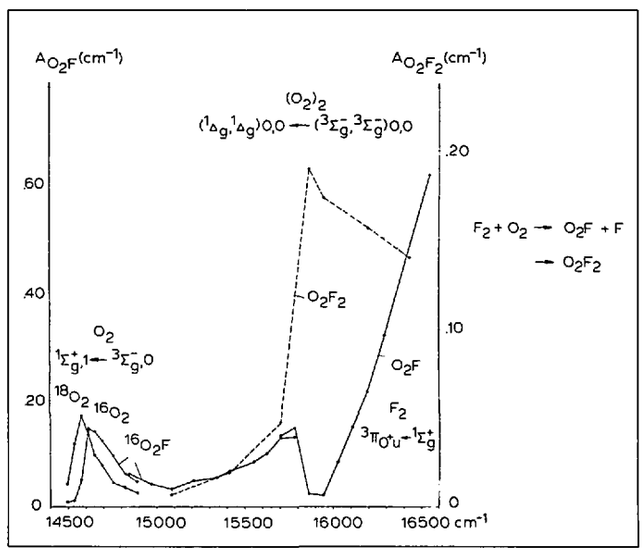

Fig. 11. *Laser-excitation spectrum of the reaction F_2+O_2 in the red-spectral range.* Each point of the O_2F curve shows the growth of the integrated absorbance of O_2F at 1493 cm^{-1} (1409 cm^{-1} in the case of $^{18}O_2F$) during an irradiation period of 15 min at 280 $mWcm^{-2}$. Each point of the O_2F_2 curve represents the growth of the integrated absorbance of O_2F_2 at 628 cm^{-1} during an irradiation period of 75 min at 350 $mWcm^{-2}$. The continuous F_2 excitation spectrum above 15000 cm^{-1} is perturbed by O_2F+F → O_2F_2 reaction induced by absorption of light by $(O_2)_2$ [39].

in our search for low-energy pathways of the reaction of O_2 with molecular fluorine. As can be seen from the excitation spectrum in *Fig. 11*, reaction could be initiated by irradiation of F_2 suspended in solid O_2 (or of $F_2 \cdot O_2$ pairs isolated in Ar matrices) at wavelengths as long as 690 nm. In this excitation spectrum, O_2F and O_2F_2 IR product growth is plotted against photolysis photon energy [39]. While the peak of the $F_2 + O_2 \rightarrow O_2F + F$ excitation spectrum around 14600 cm^{-1} signals reaction of O_2 in its $^1\Sigma_g^+$, $v = 1$ state, the monotonous increase of absorption starting around 15000 cm^{-1} towards higher energy cannot originate from O_2. We established that this continuous absorption originates from excitation to the repulsive limb of the hitherto unobserved weakly bound $^3\pi_{o+u}$ state of F_2 [40] (450 nm was the longest wavelength at which F_2 absorption had previously been reported) [41].

Optical access to this lowest triplet state of F_2 is facilitated by relief of the spin forbiddance of the $^3\pi_{o+u} \leftarrow {}^1\Sigma_g^+$ transition by the interaction of $F_2 \cdot O_2$ collisional pairs $F_2{\cdot}O_2$: $^3(^3\pi_{o+u}, {}^3\Sigma_g^-) \leftarrow {}^3(^1\Sigma_g^+, {}^3\Sigma_g^-)$ analogous to *Evans'* interpretation of oxygen enhancement of singlet-triplet absorptions of aromatics [42]. This enhancement of the highly forbidden triplet absorption of F_2 by contact with O_2 adds to the list of interactions of sustained collisional pairs that open up low-energy reaction paths that otherwise would be inaccessible.

Interesting from this perspective is also the controlled VIS-light induced photo-oxidation of tetramethylethylene in solid O_2 by *Akimoto* and coworkers [43]. Tetramethyl-1,2,3,4-tetraoxane is the sole product observed upon excitation of the long-wavelength tetramethylethylene $\cdot$ O_2 charge transfer absorption (*Scheme 8*). Although somewhat shorter wavelength, green photons are needed to initiate reaction, the high degree of product control is no doubt a result of the fact that excitation occurs into a bound state well below the dissociation limit of either reactant. More importantly, this example points to yet another type of excited state unique to sustained collisional pairs that could be exploited for controlled chemistry with NIR photons (*e.g.* chemistry of bound NIR charge transfer states of collisional pairs or complexes involving halogen molecules).

3. Redox Chemistry of NIR Energy Carriers in Solution

As mentioned briefly when presenting NIR-light-induced reactions of furan $\cdot$ O_2 collisional pairs in matrices (*2.2.2*), the $O_2(^1\Delta)$ + diene $\rightleftarrows$ endoperoxide system, coupled with a regenerative excited state redox reaction of singlet O_2 may serve as a model for temporary chemical storage of NIR photons and subsequent efficient conversion of the retrieved energy into electricity. The concept is presented in *Scheme 9*. A

Scheme 8

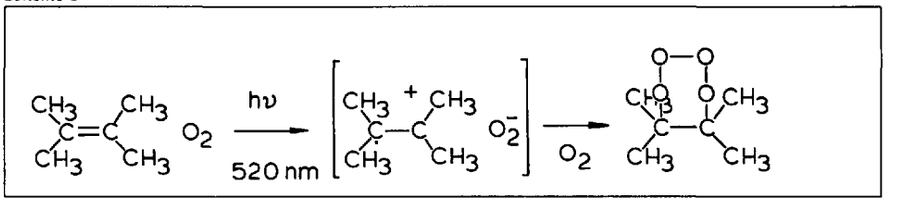

Scheme 9

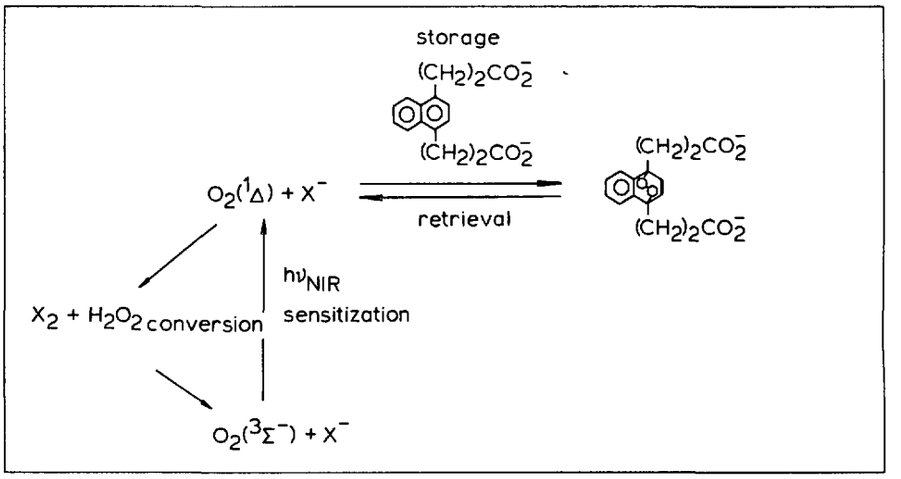

key element of the scheme is temporary chemical storage of photon energy in the form of $O_2(^1\Delta)$ stored in, and easily retrieved from, an aromatic endoperoxide molecule (right hand side of *Scheme 9*). This opens up a way to directly convert the retrieved chemical energy into electricity through a regenerative redox reaction of $O_2(^1\Delta)$ in an electrochemical cell (left hand side of *Scheme 9*), thus avoiding mere conversion of stored enthalpy into useful energy by a *Carnot* process with its intrinsic losses. Since sensitizers are available that afford very efficient transfer of absorbed long-wavelength VIS and NIR light to O_2 molecules to yield $O_2(^1\Delta)$ [35], the sequence of reactions of the proposed scheme constitutes a model for capture, temporary chemical storage, and effi-

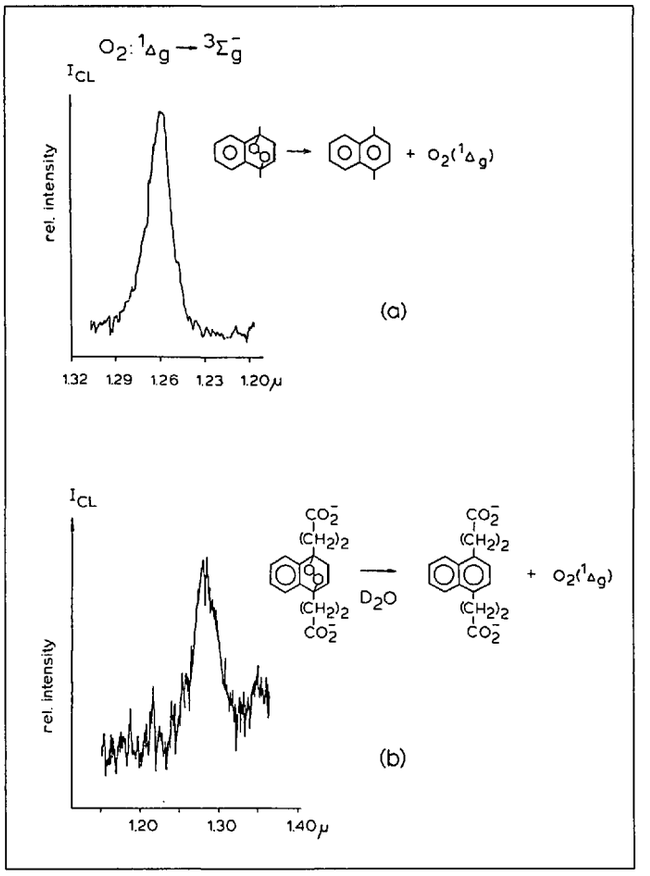

Fig. 12. *NIR thermoluminescence spectra of substituted naphthalene endoperoxides in CCl_4* (spectrum a, 22°) *and aqueous solution* (b, 65°). Signals were monitored with a very sensitive liquid N_2 cooled Ge photodiode (D* 10^{15}).

cient conversion of these photons into useful energy.

We will discuss spectroscopic studies that reveal detailed physico-chemical aspects of storage and retrieval of $O_2(^1\Delta)$ (*3.1*), of regenerative excited state redox reactions of $O_2(^1\Delta)$ in aqueous solution (*3.2*), and of direct reduction of singlet excited O_2 at a semiconductor electrode (*3.3*). In *3.4*, we will summarize our most recent work on the elucidation of detailed mechanisms of redox processes at semiconductor colloids that may play a central role in NIR-driven chemistry in solution.

3.1. *Chemical Storage of $O_2(^1\Delta)$*

Direct evidence that O_2 molecules are thermally retrieved from naphthalene endoperoxides in the $^1\Delta_g$ excited state was obtained by observation of NIR chemiluminescence at 1.3 μ [44][45]. The emission, shown in *Fig. 12a* for 1,4-dimethylnaphthalene endoperoxide decomposing in CCl_4, and in *Fig. 12b* for 3,3'-(1,4-naphthylidene)dipropionate endoperoxide decomposing in aqueous solution corresponds to the extremely weak $^1\Delta_g \rightarrow {}^3\Sigma_g^-$ phosphorescence of the eliminated O_2. In the case of 1,4-dimethylnaphthalene endoperoxide in CCl_4, we simultaneously monitored the thermal decomposition by FT-IR spectroscopy and found 1,4-dimethylnaphthalene as sole product. Hence, all spectroscopic evidence indicates that chemical storage of $O_2(^1\Delta)$ (carrying 23 kcal mol^{-1} energy) in these endoperoxides is completely reversible. As illustrated by the potential-energy diagram of the naphthalene + O_2 ⇄ endoperoxide system in *Fig. 13*, thermal expulsion of O_2 in the $^1\Delta_g$ state has its origin in spin conservation, which forces ground-state endoperoxide to decompose adiabatically on the singlet surface to ground-state hydrocarbon and $O_2(^1\Delta)$. Substituted naphthalenes as $O_2(^1\Delta)$ acceptors are of particular interest to us because the energetics of endoperoxide formation is favorable for energy storage [46] and can be fine tuned by selecting appropriate substituents.

While these steady-state phosphorescence measurements simply corroborate by direct spectroscopic observation what has been previously inferred from indirect chemical-trapping techniques in the case of decomposition of substituted anthracene endoperoxides [47], namely that O_2 is expelled in the $^1\Delta$ state, monitoring retrieved $O_2(^1\Delta)$ in real time opened up by the chemiluminescence detection technique was the real significance of this result [48]. Exploiting previous indirect evidence by *Brauer* and coworkers that aromatic endoperoxides also decompose to $O_2(^1\Delta)$ and parent hydrocarbon upon excitation to the S_2 ($\pi^* \leftarrow \pi$) state with photons above 300 nm [49], we employed ns laser-flash-chemiluminescence spectroscopy to follow the decay of $O_2(^1\Delta)$ expelled from endoperoxides for the first time [44], [45][50][51]. Monitoring in real time $O_2(^1\Delta)$ retrieved from endoperoxide storage molecules was just the method needed to explore its subsequent excited state redox chemistry.

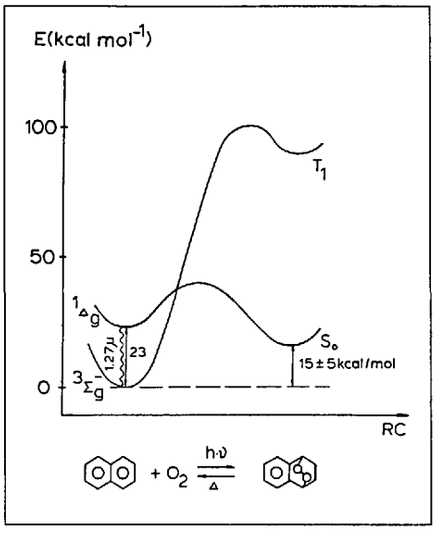

Fig. 13. *Lowest potential-energy surfaces of naphthalene+O_2 ⇄ endoperoxide system* [46]

3.2. *Reaction of $O_2(^1\Delta)$ with Iodide*

Of particular interest to us are $O_2(^1\Delta)$ reactions in aqueous solution that could be part of a regenerative redox system as proposed in *Scheme 9*: Singlet excited O_2 would react with a substrate X^- to form products which, after accumulation, would undergo spontaneous back reaction to regenerate ground state O_2. If run in an electrochemical cell configuration, such a regenerative reaction would afford, in principle, direct conversion of $O_2(^1\Delta)$ electronic energy into electrical energy. One can envision initiation of the conversion in such a cell by thermal release of $O_2(^1\Delta)$ from polymer bound endoperoxide molecules [52] located close to the cathode surface. For the immediate task of exploring $O_2(^1\Delta)$ excited-state redox reactions by time resolved spectroscopy, however, pulsed generation of singlet O_2 by ns laser flashes was required.

In contrast to the many well-established organic reactions of $O_2(^1\Delta)$ [35][36], there is very little known about aqueous inorganic redox chemistry of singlet oxygen. One inorganic reaction that has been reported sometime ago to involve singlet O_2 is photoinduced oxidation of iodide to I_3^- in aqueous solution. *Grossweiner* and coworkers [53] and *Rohatgi-Mukherjee* and *Gupta* [54] found buildup of I_3^-, when $O_2(^1\Delta)$ was generated in air-saturated aqueous iodide solution by continuous UV irradiation of a singlet-oxygen sensitizer. Although good evidence was presented for $O_2(^1\Delta)$ involvement [53], these experiments did not allow for establishment of a mechanism. Nevertheless, one group suggested that singlet O_2 does not oxidize I^- directly, but rather would form first an endoperoxide of the 2-anthracene sulfonate sensitizer employed, followed by attack of the peroxide on I^- [54]. Since oxidation of iodide by $O_2(^1\Delta)$ in neutral aqueous solution would, from a thermodynamics standpoint, constitute an ideal basis for a regenerative redox system, it was important to find out whether $O_2(^1\Delta)$ could directly oxidize I^- without sensitizer involvement and, if so, to determine the reaction steps that lead to I_3^-.

A cw Ar ion or cw dye laser-based double beam transient absorption spectrometer was employed that was equipped with a differential Si photodiode detector (*Fig. 14*). This set-up allowed us to monitor product growth in the 450–1000-nm region at a detection limit of 10^{-5}–10^{-6} absorbance units (typically 50–100 laser pulse averages). Best results were obtained when generating singlet O_2 with the sensitizer 2-anthracene sulfonate, because it kept the VIS and NIR probing region free of background absorption.

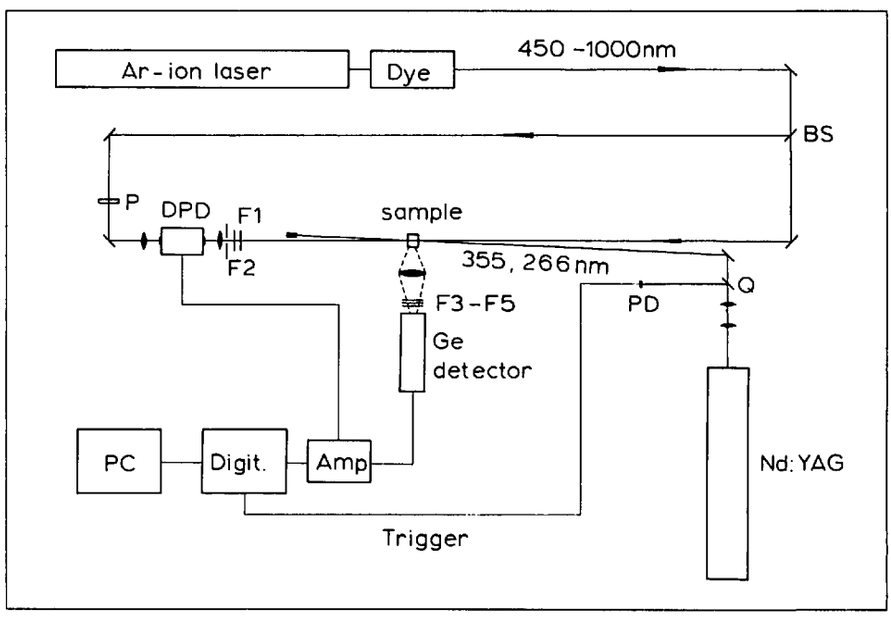

Fig. 14. *Nanosecond laser flash-emission and transient absorption-apparatus.* BS: beam splitter; P: polarizer; DPD: differential photodiode detector; Q: Quartz plate; F1, F2: Corning optical filters to protect detector from scattered UV light; F3-F5: NdGaAs, silicon, and 1.3 μ narrow band pass filters for $O_2(^1\Delta)$ phosphorescence detection.

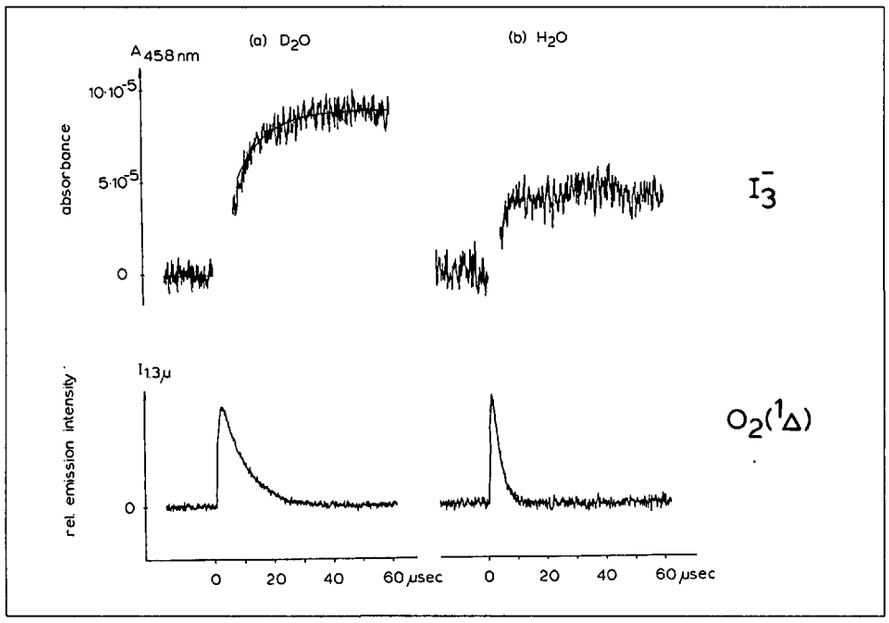

Fig. 15. *Time-resolved measurement of $O_2(^1\Delta)$+I^- reaction in aqueous solution. Top curves:* transient absorption at 458-nm observed upon 355 nm excitation of air-saturated D_2O (*a*) and H_2O (*b*) solutions containing 1.2 x 10^{-4} M 2-anthracene sulfonate and 0.1 M KI. Data points just after the laser pulse contain the strong triplet-triplet absorption of the sensitizer and are not displayed. *Bottom curves:* simultaneously measured 1.3 μ $O_2(^1\Delta)$ emission decays.

Initial experiments consisted of monitoring 1.3-μ phosphorescence decays of singlet O_2 upon pulsed 355 nm excitation of the sensitizer at various iodide concentrations, which led to a rate constant of 8.7×10^5 l mol^{-1} s^{-1} for quenching (reactive plus non-reactive) of $O_2(^1\Delta)$ by I^- in aqueous solution [55]. The bottom traces of *Fig. 15* show 1.3-μ emission decays of $O_2(^1\Delta)$ in oxygen-saturated D_2O (curve *a*) and H_2O (curve *b*) solutions containing 0.1 M I^-. A substantial solvent D-isotope effect of 2.5 on the lifetime of $O_2(^1\Delta)$ can readily be discerned from these curves. This ratio mirrors the 15 times longer lifetime of $O_2(^1\Delta)$ in neat D_2O (63 μs) than in H_2O (4 μs) [48].

The diagnostic value of the solvent D-isotope effect on the $O_2(^1\Delta)$ lifetime became fully apparent when monitoring a weak product absorption in the blue spectral range in both D_2O and H_2O solution. As can be seen from the top traces of *Fig. 15*, the rise of the absorption exhibits the same solvent D-isotope effect as the $O_2(^1\Delta)$ emission decay. This implies that the product originates from reaction of $O_2(^1\Delta)$. Measurement of the absorption signal as function of probe-laser wavelength showed that the observed product is I_3^- [55]. This data constitutes the first direct evidence for reaction of $O_2(^1\Delta)$ with I^-. The most important kinetics result regarding the reaction mechanism is that the I_3^- rise time is the same as the $O_2(^1\Delta)$ decay time at all I^- concentrations used. Observation of the I_3^- rise was only possible because of the high detection limit of the transient absorption spectrometer. The reason is that very low (< 1 mJ) laser excitation pulses (resulting in very low $O_2(^1\Delta)$ reactant concentrations) had to be used in order to prevent complete disappearance of the I_3^- signal under a triplet-triplet absorption of the singlet O_2 sensitizer that was several orders of magnitude more intense [55].

Scheme 10

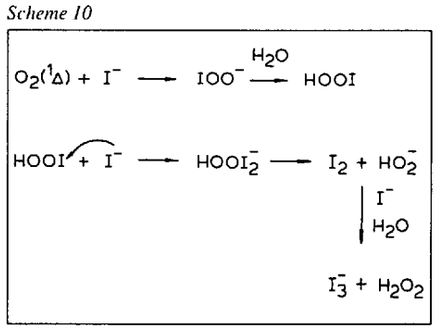

Scheme 10 shows the most probable mechanism for the $O_2(^1\Delta)$ + I^- reaction consistent with our kinetic data. A reactive encounter between $O_2(^1\Delta)$ and I^- would produce iodoperoxy anion, IOO^-. Although an intermediate that has eluded experimental observation thus far, an estimate of its pK value (*Branch-Calvin* rule [56]) suggests that this species would be completely protonated at pH = 7, on a time scale of *ca.* 100 ns according to rate constant estimates [55]. HOOI so formed is expected to decompose to I_2 and HO_2^- along the same reaction path which was proposed for HOI+I^- reaction in aqueous solution by *Eigen* and *Kustin* [57]. Namely, nucleophilic attack of I^- on HOOI to yield transient $HOOI_2^-$ at a diffusion controlled rate, followed by release of HO_2^- to give I_2 and H_2O_2. Hence, the HOOI + I^- step would proceed in no more than a few ns at the I^- concentrations used, and dissociation of $HOOI_2^-$ is expected to occur even faster than in the case of HOI_2^- which is estimated to be around 1 μs [57] (breaking of the I–O bond of $HOOI_2^-$ should be more facile than of HOI_2^- because the HO_2^- is a better leaving group than HO^-). Complexation of I_2^- by I- to give I_2- is a ns process at the I^- concentrations employed. Therefore, all proposed reaction steps following formation of IOO^- are expected to be fast on the scale of the $O_2(^1\Delta)$ lifetime, in agreement with our observation that the final product I_3^- grows at a rate equal to the singlet O_2 reactant decay. Although direct time resolved optical detection of H_2O_2 co-product would be very difficult and has indeed not been accomplished to date in iodide solution, we have established the presence of H_2O_2 by a conventional chemical test. It consists of Fe_2^+ catalyzed reaction of accumulated H_2O_2 with excess I^- to form I_3^-, monitored by steady state UV spectroscopy [55].

The energy profile of this reaction path in aqueous solution at pH = 7 is shown in *Fig. 16*. Each step is only modestly exoergic, yet the quantum efficiency of the overall reaction is quite high (15% at $[I^-]$ = 0.1 M). Important with regard to the proposed redox cycle (*Scheme 10*) is that the reverse reaction of I_3^- with H_2O_2 to regenerate ground state O_2 and I^- is spontaneous.

3.3. $O_2(^1\Delta)$ Reduction at a p-Si Electrode

A crucial objective of the proposed regenerative redox reaction of singlet oxygen (*Scheme 9*) is conversion of chemical into electrical energy in *both* the forward

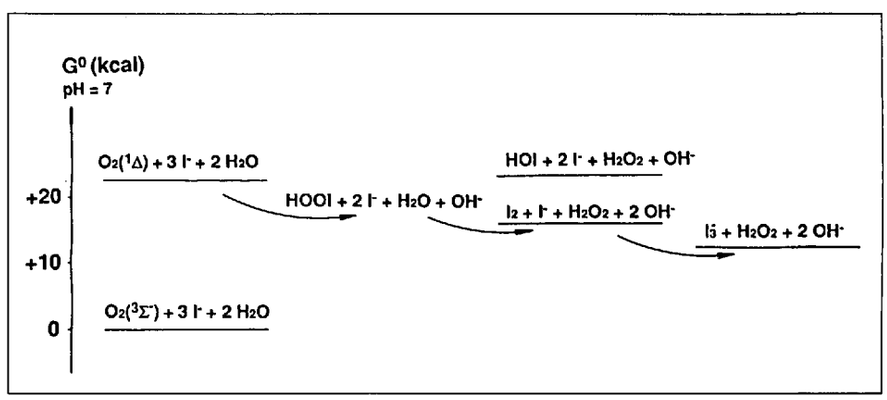

Fig. 16. *Free-energy profile of the iodoperoxy acid path of the $O_2(^1\Delta)$+I^- reaction in aqueous solution at pH = 7, determined from available standard free energies of formation* [58] *and the* Nernst *equation.* Energy of HOOI was estimated on the basis of ΔH_f^o of iodite and average bond energies [55].

($O_2(^1\Delta) + I^-$) and the reverse step ($I_3^- + H_2O_2$) so as to convert a maximum fraction of $^1\Delta$ electronic energy into electricity. While the reverse reaction involves exclusively ground-state species and could, therefore, be run in an electrochemical cell equipped with conventional electrodes, extraction of electrical energy from the $O_2(^1\Delta) + I^-$ reaction requires an electrode that would afford reduction of O_2 in its $^1\Delta$ excited state. Hence, the next key challenge in establishing the feasibility of *Scheme 9* was to demonstrate hole injection from $O_2(^1\Delta)$ into a semiconductor cathode. Electron-transfer reactions of electronically excited species at semiconductor electrodes is a very active research area whose importance for solar-energy conversion has been recognized some time ago [59], but $O_2(^1\Delta)$ reactions at such materials have not been observed thus far.

With a flat-band potential around 0 V (SCE) [60], p-type Si is a semiconductor material that has the valence band at sufficiently negative potential to afford spontaneous reduction of O_2 in the $^1\Delta$ excited state, but not in the $^3\Sigma^-$ ground state (*Scheme 11*). To find out whether reduction of $O_2(^1\Delta)$ at p-Si actually takes place, we looked for a cathodic current at a p-type single-crystal Si electrode when generating $O_2(^1\Delta)$ near the semiconductor surface. Experiments were conducted in a standard photoelectrochemical cell featuring a Si electrode immersed in an CH_3CN-electrolyte solution that contained the common $O_2(^1\Delta)$ sensitizer methylene blue (MB^+) (CH_3CN was chosen because of the long lifetime of $O_2(^1\Delta)$ in this solvent) [35]. Upon irradiation of the red absorption of MB^+ species close to the electrode surface with a continuously tunable cw dye laser, a cathodic photocurrent was observed whose spectrum agrees well with the optical absorption spectrum of methylene blue (*Fig. 17*). Maximum photocurrent was reached when suppressing back electron transfer by a 500-mV band bending introduced by cathodic polarization of the electrode [61].

The observed photocurrent spectrum shows that absorption of light by methylene blue induces a current, but that does not in itself prove that $O_2(^1\Delta)$ so produced is the species actually reduced at the p-Si electrode. However, two well established tests for involvement of $O_2(^1\Delta)$ in a chemical process confirmed that singlet O_2 was the hole injecting species and, therefore, the source of the cathodic current. First, addition of NaN_3, a well established $O_2(^1\Delta)$ quencher [35], to the electrolyte solution resulted in quenching of the photocurrent. This effect is shown in *Fig. 17* by the data points marked by a cross. The small residual photocurrent after addition of azide is due to direct bandgap excitation of p-Si by scattered laser photons (band-gap corresponds to a wavelength of 1100 nm) [62]. Second, replacing CH_3CN- by CD_3CN-electrolyte solution while keeping all other parameters the same resulted in a rise of the steady-state photocurrent by a factor of 1.7. Most convincing was that *in situ* measurement of the decay rate of $O_2(^1\Delta)$ in these electrolyte solutions by the laser flash-1.3 μ emission technique gave the same, factor of 1.7 larger lifetime in the CD_3CN than in the CH_3CN electrolyte (the solvent isotope effect in these electrolyte solutions is smaller than that in neat CH_3CN [35] because O_2^-, a very efficient $O_2(^1\Delta)$ quencher, accumulates during electrochemical runs) [61]. Hence, these results establish the feasibility of the reaction of O_2 in its $^1\Delta$ excited state at a p-type semiconductor cathode. This opens up conversion of the 1-eV electronic energy of metastable $O_2(^1\Delta)$ into electricity. A next step will be to explore materials that are thermodynamically more favorable for $^1\Delta$ electronic to electrical energy conversion (*e.g.* p-SiC), and to find conditions that allow us to use aqueous instead of CH_3CN solutions.

Apart from the significance with regard to reduction of singlet excited O_2 at a semiconductor electrode, the observed hole injection of $O_2(^1\Delta)$ into the valence band of p-Si points to semiconductor mediation of the redox chemistry of this and possibly other NIR excited molecules. Gaining access to low-energy pathways by engaging semiconductor valence or conduction bands (bulk electrode, powder, or colloid form) to mediate electron flow is particularly important in NIR-induced redox reactions because of their intrinsically low driving forces.

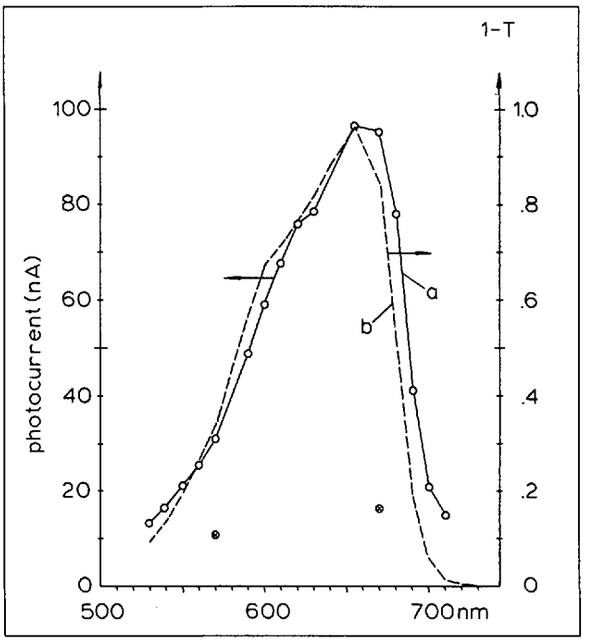

Fig. 17. a) *Photocurrent spectrum of air-saturated methylene blue solution in CH_3CN* (1.5×10^{-5} M). Electrode: p-Si, 0.16 cm^2. Laser intensity, 240 $mWcm^{-2}$. Crosses (⊗) indicate photocurrent that remains after saturating the electrolyte solution with NaN_3 ($\approx 5 \times 10^{-5}$ M). *b) Absorption spectrum of methylene blue* (1.5×10^{-5} M, pathlength = 1 cm).

Scheme 11

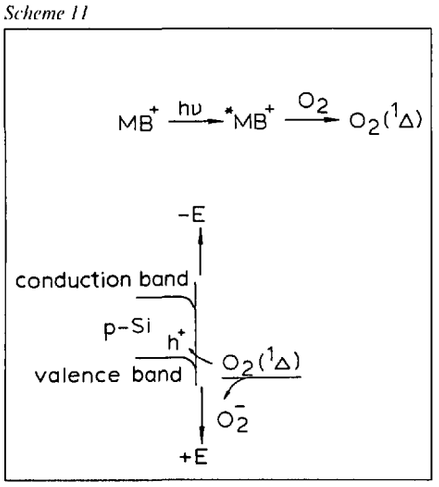

3.4. *Halide Oxidation at Sensitized Colloidal Semiconductors*

Sensitization by adsorbed dyes is a well established method of adjusting the wavelength response of semiconductor materials to the desired spectral region [59], and stable oxide semiconductors like TiO_2 have come to play a dominant role in the case of reactions of interest in solar photochemistry. While the band gap of TiO_2 itself can only be excited by near UV photons (3.2 eV), initiation of redox chemistry by injection of an electron from an adsorbed dye into the conduction band of the semiconductor has been accomplished practically at all VIS wavelengths [63]. Halide-to-halogen oxidation is one type of chemistry that has potential for chemical storage of solar photon energy and for direct-light-to-electrical-energy conversion in photodriven regenerative electrochemical cells, and here dye-sensitized TiO_2 electrodes, powders, and colloids have already proved very promising. A most recent advance are dye-loaded high surface area TiO_2 films developed by *Grätzel* and coworkers. High incident photon-to-current conversion efficiencies were observed when using such films as photoanodes in I^-/I_3^- and Br^-/Br_3^- regenerative cells [63][64].

Given the modest size of exo-ergicities of storage or regenerative reactions driven by NIR photons, knowledge of elementary reaction steps and energetics and rate of each

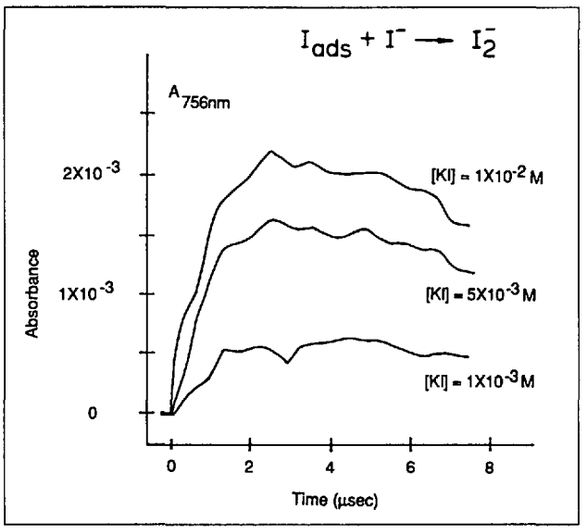

Fig. 18. *Rise of transient absorption observed upon 532-nm excitation of phenyl-fluorone-sensitized TiO_2 colloid in ethanolic iodide solution.* Probe wavelength is 756 nm. Signal is shown at three different I^- concentrations.

of them becomes essential for the design of suitable systems. We have been able to monitor the rise of the one electron oxidation intermediate I_2^- upon photo-induced iodide oxidation at sensitized colloidal TiO_2 (60-Å particles) in aqueous and ethanolic solution by laser-flash kinetic spectroscopy of its $^2\pi_g \leftarrow {}^2\Sigma_u^+$ NIR absorption, as shown in *Fig. 18* [65]. Resolution of the rise of this signal required work at I^- concentrations orders of magnitude lower than used in previous time-resolved experiments with unsensitized TiO_2 colloid [66]. This became possible only by probing in a spectral region free of sensitizer absorption, and by taking advantage of the high sensitivity of the cw-dye-laser-based double-beam spectrometer (*Fig. 14*). Sensitizing dyes employed were tris(2,2'-bipyridyl-4,4'dicarboxylate)ruthenium(II)dichloride ([RuL_3]) and 2,6,7-trihydroxy-9-phenylisoxanthen-3-one (phenylfluorone), whose interfacial electron transfer kinetics and nature of interaction with the TiO_2 surface had previously been established [67] [68]. In the case of phenylfluorone, VIS absorption and emission spectroscopy, and IR spectral studies have indicated that the sensitizer forms a chelate with the semiconductor surface as illustrated in *Scheme 12* [68].

From real time measurements like those shown in *Fig. 18*, we found that the rise of the I_2^- signal depends linearly on I^- concentration. Our preferred interpretation of this behavior is presented in *Scheme 12*. Oxidized phenylfluorone (PF^+) reacts within the duration of the 5-ns photolysis laser pulse with I^- adsorbed on the TiO_2 colloid surface to form I-atom. Adsorbed I-atoms so produced react with I^- from the solution sphere around the colloidal particle to yield I_2^-. It is this rate limiting step that is observed (*Fig. 18*). The latter disproportionates to I_3^- and I^- in the solution bulk, at a diffusion controlled rate according to I_2^- absorbance decay and I_3^- growth measurements (in the case of sensitization by RuL_3, an outer-sphere coordination complex between RuL_3 and I_2^- precedes the formation of free I_2^-) [65]. Quite surprisingly, the I_2^- yield as function of iodide concentration showed a marked deviation from a monotonous increase expected from simple *Langmuir* isotherm behavior, which we attribute to interference by an additional process, namely recapture of photo-injected conduction band electrons by transient I atoms. This process, which competes with reaction of adsorbed I-atoms with I^-, is also strongly suggested by the much lower efficiency of I^- photo-oxidation in the phenylfluorone/TiO_2 sol compared to the corresponding photoelectrochemical efficiency at an anodically polarized phenylfluorone/TiO_2 polycrystalline electrode [68]. Moreover, the data can only be explained by assuming a substantial spread in the efficiency by which adsorbed I-atoms recapture conduction-band electrons. This implies that iodide photo-oxidation efficiencies in sensitized colloids depend critically on the specific site on the TiO_2 surface at which the primary photooxidation product (I-atom) is formed [65].

Scheme 12

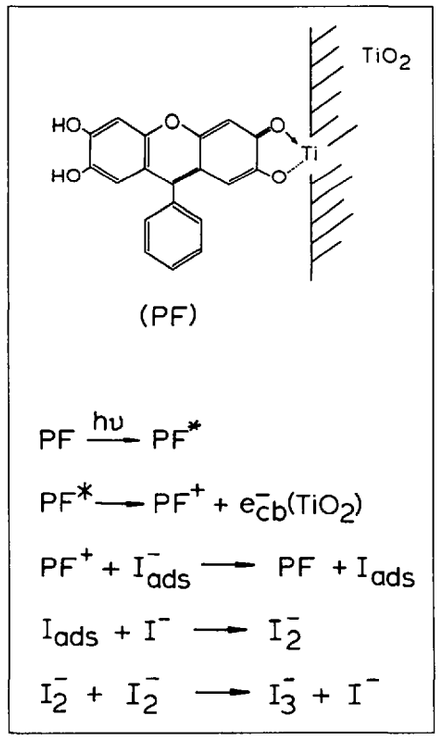

4. Conclusions

Beyond new results in specific areas, such as elucidation of stereochemical details of hydrocarbon oxidation paths, synthesis of strained episulfoxides by singlet SO chemistry, or detection of very weak NIR vibronic absorptions by laser-reaction-excitation spectroscopy, the most general finding of our photochemical work in solid matrices is the high product specificity of red- and NIR-induced bimolecular reactions. Several factors have been brought to light by the systems studied thus far. Excess internal energy of primary transient photoproducts is one key factor, most clearly manifested in the results of alkene and alkyne photo-oxidation by NO_2. There, simultaneous monitoring of the structure of the transient biradical (by chemical trapping in its nascent conformation) and tuning of its excess energy (by selection of the photolysis wavelength) revealed how internal energy acquired by the transient can alter its chemistry and hence the distribution of final products. The NO_2 work also showed us how crucial it is to avoid photolysis above the reactant dissociation threshold. Indeed, we consider the special opportunity, in terms of product specificity, of chemistry along large-amplitude reaction paths accessed by long-wavelength photons as the most interesting result of these studies. Several different types of excited states unique to sustained collisional pairs (or weak complexes) that can be exploited for controlled chemistry have been encountered thus far, and there is no doubt that more will be found as new systems are explored.

Main emphasis in our time-resolved work on chemical storage of singlet O_2 and its redox chemistry in homogeneous solution and at semiconductors has been on direct optical monitoring of reactants and products, which required substantial improvement of the sensitivity for $O_2(^1\Delta)$ and redox-product detection. Aside from new mechanistic insight gained in these studies, the improved detection methods are important progress as they are indispensable for further exploration of long-wavelength light induced redox chemistry, particularly in semiconductor sols. Our initial results in the latter area indicate that even for a reaction as simple as halide oxidation the competing processes at the semiconductor-solution interface are complex. Yet it is the understanding of these processes that is our best chance for progress in semiconductor-mediated NIR redox chemistry.

While the relevance of the mechanistic studies on singlet O_2 and halide redox chemistry with respect to NIR energy stor-

age and conversion has already been pointed out in *Sect. 3*, possible implications of long-wavelength photo-induced bimolecular reactions in solid matrices deserves further comment. Can we exploit the unique photochemistry of collisional pairs in a solid matrix for synthesis of high valued chemicals using long-wavelength sunlight (or even light from artificial sources as red and NIR photons are the least expensive ones to generate artificially)? Stereospecific alkene photo-epoxidation by NO_2 has attributes that make it an interesting case to think about: nitric oxide co-product can easily be re-oxidized by O_2 to NO_2 in the room temperature gas phase, hence one can envision red-light-induced O-atom transfer from NO_2 to alkenes in a solid matrix as the central step of a photo-assisted catalytic scheme for alkene epoxidation in which NO is the catalyst and O_2 is the oxidant actually consumed. Product-specific catalytic oxidation of small, unfunctionalized hydrocarbons that use O_2 as terminal oxidant is currently a key challenge in catalysis research [69]. Photo-assisted catalytic processes are particularly attractive for chemical synthesis as no thermal activation is required, which minimizes loss of product specificity (in particular stereospecificity) due to thermal rearrangement of primary products. Ideally, processes would be conducted in a room temperature environment, hence the question is whether a reaction like olefin epoxidation could be conducted in a room temperature solid matrix. Can one, *e.g.*, dope a room temperature polymer matrix with a transition-metal complex featuring NO_2 as ligand, and then effect controlled O-atom transfer to small alkenes, loaded into the matrix, by irradiating it with red or NIR-light? Although we are only just beginning to take steps towards this goal, the need to explore such possibilities and to rethink the role of photo-assisted chemical synthesis is clear in view of emerging demands for new synthetic routes of large-volume chemicals that meet stringent requirements in terms of exclusion of side products, efficient and sustainable use of environmentally acceptable feedstocks, and energy efficiency.

It is my pleasure to acknowledge past and present coworkers whose work has been discussed in this article, *James Harrison, Shobi Khan*, Drs. *Geir Braathen, Pi-Tai Chou, Donald Fitzmaurice, Munetaka Nakata, Farid Salama*, and *Kazuhiko Shibuya*. I thank Prof. *Michael Grätzel* for initiating work on semiconductor colloids and photo-electrochemical studies during his sabbatical stay in our laboratory. I am particularly thankful to the late Prof. *George C. Pimentel*, my mentor in Berkeley. This work was supported by the Director, Office of Energy Research, Office of Basic Energy Sciences, Chemical Sciences Division of the U.S. Department of Energy under Contract No. DE-AC03-76-SF00098.

Received: February 22, 1991

[1] J. R. Bolton, *Science* **1978,** *202*, 705; E. Schumacher, *Chimia* **1978,** *32*, 193; T. E. Casti, J. W. Otvos, *J. Chem. Educ.* **1986,** *63*, 35.

[2] G. C. Pimentel, in 'Formation and Trapping of Free Radicals', Eds. A. M. Bass and H. P.Broida, Academic Press, New York, 1960, p. 109; H. E. Hallam, Ed., 'Vibrational Spectroscopy of Trapped Species', Wiley, New York, 1973; M. J. Almond, A. J. Downs, 'Spectroscopy of Matrix Isolated Species in: Advances in Spectroscopy 17', Eds. R. J. H. Clark and R. E. Hester, Wiley, New York, 1989; L. Andrews, M. Moskovits, Ed., 'Chemistry and Physics of Matrix Isolated Species', Elsevier, Amsterdam, 1989.

[3] M. Nakata, H. Frei, *J. Am. Chem. Soc.* **1989,** *111*, 5240.

[4] D. K. Hsu, D. L. Monts, R. N. Zare; 'Spectral Atlas of Nitrogen Dioxide', Academic Press, New York, 1978.

[5] K. Mislow, 'Introduction to Stereochemistry', Benjamin, New York, 1965, p. 127.

[6] M. Nakata, H. Frei. *J. Phys. Chem.* **1989,** *93*, 7670.

[7] T. Fueno, Y. Takahara, K. Yamaguchi, 'Proceedings of the Symposium on Molecular Structure', Chem. Soc. Jpn. Tokyo, 1986.

[8] M. Dupuis, J. J. Wendoloski, T. Takada, W. A. Lester, Jr., *J. Chem. Phys.* **1982,** *76*, 481.

[9] W. A. Lester, Jr., M. Dupuis, T. J. O'Donnell, A. J. Olsen, 'Frontiers in Chemistry', Ed. K. J. Laidler, Pergamon Press, New York, 1982, p. 159.

[10] M. Nakata, K. Shibuya, H. Frei, *J. Phys. Chem.* **1990,** *94*, 8168.

[11] M. Nakata, H. Frei, *J. Chem. Soc. Jpn.* **1989,** 1412.

[12] D. J. Fitzmaurice, H. Frei, to be published.

[13] P. J. Robinson, K. A. Holbrook, 'Unimolecular Reactions', Wiley, New York, 1972.

[14] D. J. Fitzmaurice, H. Frei, *J. Phys. Chem.* **1991,** *95*, 2652.

[15] M. R. Imam, N. L. Allinger, *J. Mol. Struct.* **1985,** *126*, 345.

[16] A. J. Barnes, Ed., 'Matrix Isolation Spectroscopy', Reidel, Dortrecht, 1981, p. 531.

[17] In earlier work on the steric course of free radical attack on substituted cyclohexenes (E. S. Huyser, J. R. Jeffrey, *Tetrahedron* **1965,** *21*, 3083; O. Simamura, in 'Topics in Stereochemistry 4', Eds. E. L. Eliel and N. L. Allinger, Wiley, New York, 1969, p. 1), partial stereospecificity observed upon approach of the C=C bond from the two sides has been interpreted, in part, by formation of TB-a and CH-a along paths corresponding to the left and right path in *Fig. 6*, respectively. Although transient formation of TB conformers would be consistent with experimental data, the stereochemical course of the reactions can be rationalized even in this case without assuming intermediacy of unstable TB conformers.

[18] R. J. Cvetanovic, D. L. Singleton, *Rev. Chem. Intermed.* **1984,** *5*, 183.

[19] R. Withnall, L. Andrews, *J. Phys. Chem.* **1987,** *91*, 784; B. W. Moores, L. Andrews, *ibid.* **1989,** *93*, 1902; L. Andrews, M. Moskovits, Ed., 'Chemistry and Physics of Matrix Isolated Species', Elsevier, Amsterdam, 1989, p. 42.

[20] S. A. Abrash, G. C. Pimentel, *J. Phys. Chem.* **1989,** *93*, 5828; *ibid.* **1989,** *93*, 5834.

[21] C. Wittig, S. Sharpe, R. A. Beaudet, *Acc. Chem. Res.* **1988,** *21*, 341; S. K.Shin, Y. Chen, S. Nickolaisen, S. W. Sharpe, R. A. Beaudet, C. Wittig, *Adv. Photochem.*, in press.

[22] J. J. Havel, *J. Am. Chem. Soc.* **1974,** *96*, 530.

[23] E. G. Lewars, *Chem. Rev.* **1983,** *83*, 519.

[24] M. Nakata, H. Frei, submitted.

[25] J. A. Harrison, H. Frei, in preparation.

[26] J. March, 'Advanced Organic Chemistry', 3rd edn., Wiley, New York, 1985, p. 175.

[27] R. Atkinson, S. M. Aschmann, A. M. Winer, J. N. Pitts, Jr., *Int. J. Chem. Kin.* **1984,** *16*, 697; T. Ohta, H. Nagura, S. Suzuki, *ibid,* **1986,** *18*, 1; H. Shechter, *Rec. Chem. Prog.* **1964,** *25*, 55; D. H. Giamalva, G. B. Kenion, D. F. Church, W. A. Pryor, *J. Am. Chem. Soc.* **1987,** *109*, 7059. In the case of the reaction in solution, an additional path involving abstraction of allylic hydrogen is observed.

[28] I. Barnes, K. H. Becker, E. H. Fink, *Chem. Phys. Lett.* **1979,** *67*, 310; R. Colin, *Can. J. Phys.* **1968,** *46*, 1539.

[29] M. A. A. Clyne, A. J. MacRobert, *Int. J. Chem. Kinet.* **1981,** *13*, 187; W. B. DeMore, J. J. Margitan, M. J. Molina, R. T. Watson, D. M. Golden, *ibid.* **1985,** *17*, 1135; R. M. Dodson, R. F. Sauers, *Chem. Commun.* **1967,** 1189; *ibid.* **1969,** 1159; Y. L. Chow, J. N. Tam, J. E. Blier, H. H. Szmant, *ibid.* **1970,** 1604; P. Chao, D. M. Lemal, *J. Am. Chem. Soc.* **1973,** *95*, 920; *ibid.* **1973,** *9*, 922.

[30] L. Salem, 'Electrons in Chemical Reactions: First Principles', Wiley, New York, 1982.

[31] F. Salama, H. Frei, *J. Phys. Chem.* **1989,** *93*, 1285.

[32] N. J. Turro, 'Modern Molecular Photochemistry', Benjamin, Menlo Park, 1978, p. 414.

[33] G. Herzberg, 'Spectra of Diatomic Molecules', Van Nostrand, New York, 1950, p. 446.

[34] K. P. Crone, K. J. Kugler, *Chem. Phys.* **1985,** *99*, 293.

[35] D. Bellus, *Adv. Photochem.* **1979,** *11*, 105; F. Wilkinson, J. G. Brummer, *J. Phys. Chem. Ref. Data* **1981,** *10*, 809; A. A. Frimer, Ed., 'Singlet O_2', CRC Press, Boca Raton, 1985, Vols. I–III.

[36] H. H. Wasserman, R. W. Murray, Eds., 'Singlet Oxygen', Academic Press, New York, 1979.

[37] H. Frei, G. C. Pimentel, *J. Chem. Phys.* **1983,** *79*, 3307; H. Frei, G. C. Pimentel, in 'Chemistry and Physics of Matrix Isolated Species', Eds. L. Andrews and M. Moskovits, Elsevier, Amsterdam, 1989, Chapt. 6.

[38] R. Bhandari, L. M. Falikov, *J. Phys. C* **1973,** *6*, 479.

[39] H. Frei, *J. Chem. Phys.* **1984,** *80*, 5616.

[40] D. C. Cartwright, P. J. Hay, *J. Chem. Phys.* **1979,** *70*, 3191.

[41] E. A. Colbourn, M. Dagenais, A. E. Douglas, J. W. Raymonda, *Can. J. Phys.* **1976,** *54*, 1343; R. K. Steunenberg, R. C. Vogel, *J. Am. Chem. Soc.* **1956,** *78*, 901.

[42] D. F. Evans, *J. Chem. Soc.* **1953,** 345; *ibid.* **1957,** 1351, 3885; *ibid.* **1959,** 2753.

[43] S. Hashimoto, H. Akimoto, *J. Phys. Chem.* **1986,** *90*, 529.

[44] P.-T. Chou, H. Frei, *Chem. Phys. Lett.* **1985,** *122*, 87.

[45] P.-T. Chou, S. Khan, H. Frei, *Chem. Phys. Lett.* **1986,** *129*, 463.

[46] B. Stevens, S. R. Perez, J. A. Ors, *J. Am. Chem. Soc.* **1974,** *96*, 6846; M.Schaeffer, U. Brocker, E. Vogel, *Angew. Chem.* **1976,** *88*, 266.

[47] A. M. Trozzolo, S. R. Fahrenholtz, *Ann. N. Y. Acad. Sci.* **1970,** *171*, 61; H. H. Wasserman, D. L. Larsen, *J. Chem Soc., Chem. Commun.* **1972,** 253; H. H. Wasserman, J. R. Scheffer, J. L. Cooper, *J. Am. Chem. Soc.* **1972,** *94*, 4991; N. J. Turro, M. F. Chow, *ibid.* **1979,** *101*, 3701; I. Saito, T. Matsuura, in 'Singlet Oxygen', Eds. H. H. Wasserman and R. W. Murray' Academic Press, New York, 1979, p. 511.

[48] 1.3-μ emission of singlet O_2 generated by photosensitization in solution has first been observed by A. U. Khan, M. Kasha, *Proc. Natl. Acad. Sci. U.S.A* **1979,** 76, 6047; A. A. Krasnovsky, Jr., *Photochem. Photobiol.* **1979,** *29*, 29. Lifetime measurements based on photosensitized emission were first reported by: K. I. Salokhiddinov, D. M. Dzhagarov, I. M. Byteva, G. P. Gurinovich, *Chem. Phys. Lett.* **1980,** *76*, 85; J. R. Hurst, J. D. McDonald, G. B. Schuster, *J. Am. Chem. Soc.* **1982,** *104*, 2065; J. G. Parker, W. D. Stanbro, *ibid.* **1982,** *104*, 2067; P. R. Ogilby, C. S. Foote, *ibid.* **1982,** *104*, 2069; M. A. J. Rodgers, P. T. Snowden, *ibid.* **1982,** *104*, 5541.

[49] R. Schmidt, K. Schaffner, W. Trost, H. D. Brauer, *J. Phys. Chem.* **1984,** *88*, 956.

[50] P.-T. Chou, H. Frei, *J. Chem. Phys.* **1987,** *87*, 3843.

[51] K. B. Eisenthal, N. J. Turro, C. G. Dupuy, D. A. Hrovat, J. Langan, T. A. Jenny, E. V. Sitzmann, *J. Phys. Chem.* **1986,** *90*, 5168; This paper reports time resolved (ps) decomposition of endoperoxides by LIF detection of the hydrocarbon fragment. See also: T. Blumenstock, F. J. Comes, R. Schmidt, H. D. Brauer, *Chem. Phys. Lett.* **1986,** *127*, 452.

[52] I. Saito, R. Nagata, T. Matsuura, *Tetrahedron Lett.* **1981,** *22*, 4231; *J. Am. Chem. Soc.* **1985,** *107*, 6329.
[53] A. G. Kepka, L. I. Grossweiner, *Photochem. Photobiol.* **1971,** *14*, 621; *ibid.* **1973,** *18*, 49; W. Poppe, L. I. Grossweiner, *ibid.* **1975,** *22*, 217.
[54] K. K. Rohatgi-Mukherjee, A. K. Gupta, *Chem. Phys. Lett.* **1977,** *46*, 368; *Photochem. Photobiol.* **1978,** *27*, 539.
[55] G. Braathen, P.-T. Chou, H. Frei, *J. Phys. Chem.* **1988,** *92*, 6610.
[56] W. L. Jolly, 'Modern Inorganic Chemistry', McGraw-Hill, New York, 1984, p. 181.
[57] M. Eigen, K. Kustin, *J. Am. Chem. Soc.* **1962,** *84*, 1355.
[58] A. J. Bard, R. Parsons, J. Jordan, 'Standard Potentials in Aqueous Solution', Marcel Dekker, New York, 1985.
[59] H. Gerischer, F. Willig, in 'Topics in Current Chemistry 61', Ed. F. Boschke, Springer Verlag, Berlin, 1976, p. 31; T. Watanabe, A Fujishima, K. Honda, in 'Energy Resources through Photochemistry and Catalysis', Ed. M. Grätzel, Academic Press, New York, 1983, p. 359; R. Memming, *Progr. Surface Sci.* **1984,** *17*, 7.
[60] J. A. Turner, J. Manassen, A. J. Nozik, *Appl. Phys. Lett.* **1980,** *37*, 488; D. Laser, A. J. Bard, *J. Phys. Chem.* **1976,** *80*, 459.
[61] M. Grätzel, H. Frei, *J. Phys. Chem.* **1989,** *93*, 7037.
[62] A. J. Nozik, *Annu. Rev. Phys. Chem.* **1978,** *29*, 189.
[63] N. Vlachopoulos, P. Liska, J. Augustynski, M. Grätzel, *J. Am. Chem. Soc.* **1988,** *110*, 1216, and ref. cit. therein.
[64] P. Liska, N. Vlachopoulos, M. K. Nazeeruddin, P. Compte, M. Grätzel, *J. Am. Chem. Soc.* **1988,** *110*, 3686; P. Compte, M. K. Nazeeruddin, F. P. Rotzinger, A. J. Frank, M. Grätzel, *J. Mol. Catal.* **1989,** *52*, 63.
[65] D. J. Fitzmaurice, H. Frei, *Langmuir* **1991,** *7*, ...
[66] A. Henglein, *Ber. Bunsenges. Phys. Chem.* **1982,** *86*, 241; J. Moser, M. Grätzel, *Helv. Chim. Acta* **1982,** *65*, 1436.
[67] J. Desilvestro, M. Grätzel, L. Kavan, J. Moser, *J. Am. Chem. Soc.* **1985,** *107*, 2988.
[68] H. Frei, D. J. Fitzmaurice, M. Grätzel, *Langmuir* **1990,** *6*, 198.
[69] Conference Report by J. Haggin, *C&E News* Aug. 31 **1987,** 18; Sept. 3 **1990,** 30; R. A. Sheldon, J. K. Kochi, 'Metal-Catalyzed Oxidations of Organic Compounds, Academic Press', New York, 1981.

Chimia 45 (1991) 190–193

Allocution prononcée à l'occasion de la remise du *Prix Latsis* 1990

le 19 novembre 1990 au Rathaus de Berne

Geoffrey Bodenhausen*

Monsieur le Conseiller fédéral,
Mesdames, Messieurs,
Chers arnis,

Contrairement à mes habitudes, je vous ai préparé un texte écrit, afin de partager avec vous quelques réflexions. J'ai une fois eu le plaisir d'écouter le très éloquent physico-chimiste *Peter Atkins* qui commencait son discours *ainsi: 'If you think that I am reading from a piece of paper, well, that's precisely what I shall be doing'*.

C'est d'abord une source de grande satisfaction de savoir que ce Prix n'est pas d'office destiné à un chimiste. En effet, cela vaut bien plus qu'une récompense attribuée par une association professionnelle à l'un de ses membres. Un prix de chimiste signalerait tout au plus que l'on jouit de la confiance de quelques collègues immédiats. Or ce *Prix Latsis* est d'une autre catégorie, et je m'en réjouis. Entendez-moi bien: je ne me fais pas d'illusions. Je me rends parfaitement compte qu'il est bien difficile – voire impossible – de comparer les mérites d'un mathématicien, d'un ingénieur ou d'un physico-chimiste. Je pense qu'il y a d'autres candidats en Suisse dont le mérite est au moins égal au mien, et je ne doute pas qu'il y ait un élément d'arbitraire – et partant d'injustice – dans le choix d'un candidat.

Cependant, je suis heureux de voir ce prix attribué à un chimiste. Je pense d'abord à la chimie au sens large, qu'elle soit analytique ou synthétique, qu'elle soit propre ou polluante, qu'elle soit traditionnelle ou qu'elle se situe à la lisière de spécialités modernes telles que la biologie moléculaire. Cette chimie représente un domaine extraordinairement vaste, d'une richesse indescriptible, qui est le théâtre d'un foisonnement d'idées d'une grande variété. Je crois que cette richesse est tout à fait inconnue du grand public.

Songez donc par exemple: quelle incroyable latitude s'offre à un enseignant universitaire lorsqu'il établit le programme d'un cours de chimie! Pour les uns, la pratique de la chimie est un métier essentiellement manuel, un artisanat au sens noble du terme, qui requiert avant tout de l'adresse et de la débrouillardise. Pour d'autres (et je me situe plutôt parmi ceux-là), cette même chimie est une activité plutôt intellectuelle, qui se pratique un crayon à la main, à la rigueur à l'aide d'un ordinateur. J'avoue que je n'ai plus tenu d'éprouvette dans les mains depuis plus de quinze ans. Est-ce à dire que je suis un renégat, un chimiste qui s'est subrepticement recyclé en physicien? Point du tout! Je crois que, malgré la fâcheuse tendance au morcellement, la chimie demeure une science essentiellement indivisible.

Si je prends la défense de la chimie aujourd'hui, c'est parce que je la sens mal aimée et incomprise. La presse ne parle que pollution, elle ne s'intéresse à la chimie que s'il y a un accident à déplorer, elle se borne trop souvent à refléter la fascination bien humaine (et un brin morbide) devant le danger. A lire certains articles, on serait parfois amené à croire que les chimistes sont personnellement responsables du fait que la combustion du pétrole dégage du gaz carbonique!

Alexandre Vialatte a dit (à propos de la langue française et de son orthographe): «*Quand on est amoureux de sa langue, on l'aime dans ses difficultés. On l'aime telle quelle, comme sa grand 'mère, avec ses rides et ses verrues.*» C'est dans ce sens que je vois la chimie, que je revendique mon appartenance à cette communauté scientifi-

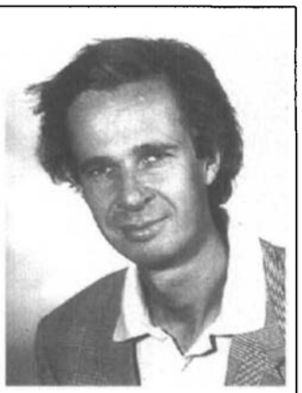

Geoffrey Bodenhausen: né le 7 mai 1951 à La Haye, Pays-Bas. Ecole primaire à La Haye, Pays-Bas. Ecole Internationale de Genève, 1963–1970 (Maturité fédérale type C). Ecole polytechnique fédérale de Zürich, 1970–1974 (Diplôme de chimie). Thèse de doctorat sous la direction du Prof. *Ray Freeman*, Laboratoire de chimie physique, Université d'Oxford, 1975–77 (D.Phil.). Scholarship of the Salter's Company, London, 1976–77. University of California at San Diego, 1978: Recherches en spectroscopie à multiples quanta (Prof. *R.L. Vold* et *R.R. Vold*). Member of Research Staff, Francis Bitter National Magnet Laboratory, Massachusetts Institute of Technology, 1979–1980: Recherches en résonance magnétique des substances solides. Assistant, puis maître-assistant, Laboratoire de chimie physique, Ecole polytechnique fédérale de Zürich, 1980–1985: Enseignement en chimie physique, rédaction d'une monographie et recherches variées en spectroscopie. Prix 1983 de l'Association des chimistes suisses. Privat-docent en chimie physique, Ecole polytechnique fédérale de Zürich, 1984–88. Professeur associé, Institut de chimie organique, Université de Lausanne, 1985 – présent. Directeur, Institut de chimie organique, sept. 1987 – déc. 1990. *Prix Latsis 1990* décerné par le Fonds national de la recherche scientifique.

*Correspondance: Prof. G. Bodenhausen
Section de Chimie
Université de Lausanne
Rue de la Barre 2
CH-1005 Lausanne